HHS Public Access

Author manuscript

J Neurochem. Author manuscript; available in PMC 2021 July 01.

Published in final edited form as:

J Neurochem. 2020 July ; 154(2): 158–176. doi:10.1111/jnc.14966.

Expression of α3β2β4 nicotinic acetylcholine receptors by rat adrenal chromaffin cells determined using novel conopeptide antagonists

Arik J. Hone[1,2,5], **Lola Rueda-Ruzafa**[3,5], **Thomas J. Gordon**[2], **Joanna Gajewiak**[2], **Sean Christensen**[2], **Tino Dyhring**[4], **Almudena Albillos**[5], **J. Michael McIntosh**[1,2,6]

[1]George E. Whalen Veterans Affairs Medical Center, Salt Lake City, Utah, USA

[2]School of Biological Sciences, University of Utah, Salt Lake City, Utah, USA

[3]Biomedical Research Center (CINBIO), University of Vigo, Vigo, Spain

[4]Saniona A/S, Ballerup, Denmark

[5]Departament of Pharmacology and Therapeutics, Universidad Autónoma de Madrid, Madrid, Spain

[6]Department of Psychiatry, University of Utah, Salt Lake City, Utah, USA.

Abstract

Adrenal chromaffin cells release neurotransmitters in response to stress and may be involved in conditions such as post-traumatic stress and anxiety disorders. Neurotransmitter release is triggered, in part, by activation of nicotinic acetylcholine receptors (nAChRs). However, despite decades of use as a model system for studying exocytosis, the nAChR subtypes involved have not been pharmacologically identified. Quantitative real-time PCR of rat adrenal medulla revealed an abundance of mRNAs for α3, α7, β2, and β4 subunits. Whole-cell patch-clamp electrophysiology of chromaffin cells and subtype-selective ligands were used to probe for nAChRs derived from the mRNAs found in adrenal medulla. A novel conopeptide antagonist, PeIA-5469, was created that is highly selective for α3β2 over other nAChR subtypes heterologously expressed in *Xenopus laevis* oocytes. Experiments using PeIA-5469 and the α3β4-selective α-conotoxin TxID revealed that rat adrenal medulla contain two populations of chromaffin cells that express either α3β4 nAChRs alone or α3β4 together with the α3β2β4 subtype. Conclusions were derived from observations that acetylcholine-gated currents in some cells were sensitive to inhibition by PeIA-5469 and TxID, while in other cells, currents were sensitive only to TxID. Expression of functional α7 nAChRs was determined using three α7-selective ligands: the agonist PNU282987, the positive allosteric modulator PNU120596, and the antagonist α-conotoxin [V11L,V16D]ArIB. The results

Corresponding Author: Arik J. Hone PhD, uuneurotox@yahoo.com, School of Biological Sciences, University of Utah, Salt Lake City, Utah 84112 and J. Michael McIntosh M.D., School of Biological Sciences and the Department of Psychiatry, University of Utah, Salt Lake City, Utah 84112, mcintosh.mike@gmail.com.

Author contributions

A.J. Hone designed and performed research, analyzed data, and wrote the paper; L. Rueda-Ruzafa performed research and analyzed data; T.J. Gordon performed research and analyzed data; J. Gajewiak performed research and analyzed data; S. Christensen performed research and analyzed data; T. Dyhring contributed new reagents; A. Albillos wrote the paper; J.M. McIntosh wrote the paper.

The authors declare there are no conflicts of interest.

of these studies identify for the first time the expression of α3β2β4 nAChRs as well as functional α7 nAChRs by rat adrenal chromaffin cells.

Graphical Abstract

Adrenal chromaffin cells are an important secretory cell type and responsible for the homeostasis of a host of physiological functions. The nicotinic acetylcholine receptors (nAChRs) expressed by these cells are critical players in the secretion-coupling response and the release of catecholamines and other neurotransmitters into the bloodstream. Despite decades of use as a model system, the nAChRs subtypes expressed by rat chromaffin cells have not been fully elucidated. Here we report that chromaffin cells express three main nAChR subtypes: α3β2β4, α3β4, and α7. This study provides significant advances in our understanding of the nAChR expression profile of rat chromaffin cells.

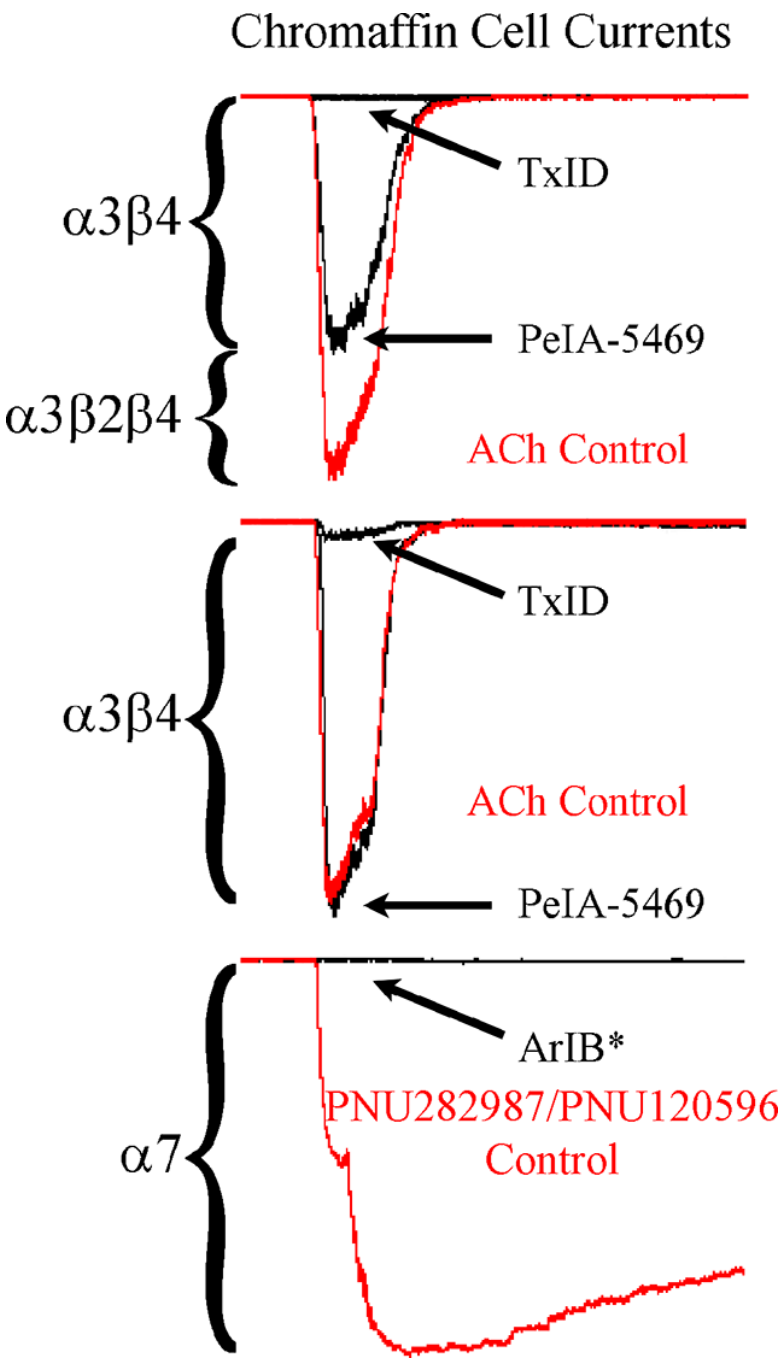

Keywords

adrenal chromaffin cell; nicotinic acetylcholine receptor; α-conotoxin; pituitary gland

INTRODUCTION

The adrenal medulla is classically thought of as the flight-or-fight organ of the body whose function is to release catecholamines into the bloodstream in response to stressful stimuli

and to maintain homeostasis of a host of bodily functions. This perhaps overly simplistic view has been challenged by the discovery that the secretory cell of the adrenal medulla, the chromaffin cell, releases a variety of substances in addition to catecholamines including other small molecules and neuropeptides (Eiden & Jiang 2018; Podvin *et al.* 2015). One such neuropeptide, called pituitary adenylate cyclase-activating polypeptide (PACAP), has been proposed to be a 'stress-transducer neurotransmitter' (Eiden *et al.* 2018; Eiden & Jiang 2018). Studies in humans with post-traumatic stress disorder (PTSD) have found an association between having a PTSD diagnosis and mutation in the PACAP receptor PAC1 (Ressler *et al.* 2011; Lind *et al.* 2017). PACAP is released from the splanchic nerve during high frequency stress-related firing, but not during tonic, low frequency basal-rate firing, and induces catecholamine release from chromaffin cells (Kuri *et al.* 2009; Stroth *et al.* 2013). PACAP has been shown to enhance the sensitivity of nicotinic acetylcholine receptors (nAChRs) to acetylcholine (ACh) (Pardi & Margiotta 1999) and has been proposed to be co-released along with ACh by the splanchnic nerve at the adrenomedullary synapse (Hamelink *et al.* 2002).

In contrast to the action-potential (AP)-independent release of catecholamines evoked by PACAP, ACh-induced release is AP-dependent. Activation of chromaffin cell nAChRs by ACh depolarizes the membrane to elicit APs and facilitate the entry of calcium as part of the stimulus-secretion coupling response (Brandt *et al.* 1976; Douglas *et al.* 1967; Douglas & Rubin 1961; Biales *et al.* 1976). The entry of calcium via a diverse population of calcium channels promotes the fusion of vesicles with the cell membrane to trigger exocytosis (Garcia *et al.* 2006; Mahapatra *et al.* 2012; Perez-Alvarez *et al.* 2008). The role of ACh and nAChRs in the stimulus-secretion coupling response of chromaffin cells has been well documented (Perez-Alvarez & Albillos 2007), but despite decades of use as a model system for studying secretory processes (Neher & Marty 1982; Douglas 1968; Livett *et al.* 1983), pharmacological identification of the nAChR subtypes expressed by chromaffin cells using subtype-specific ligands is lacking. With the development of new therapeutic drugs that target nAChRs, it may be critical to identify the nAChR subtypes expressed by these cells in order to avoid off-target drug activity on chromaffin cell nAChRs which might negatively alter the release of neurotransmitters and provoke unwanted secondary side effects.

nAChRs are ligand-gated ion channels that are formed from a diverse number of individual subunits (Dani 2015). There are 17 (α1-α10, β1-β4, δ, ε, γ) of these subunits that assemble together in pentameric fashion to produce different receptor/ion channel subtypes, each with distinct but overlapping pharmacological and biophysical properties. In many cases, a given cell type may express numerous nAChRs making causal correlations between specific subtypes and cellular processes challenging. For example, dorsal root ganglion neurons have been shown to express several subtypes including α3β4* (the asterisk denotes the known or potential presence of other subunits in native nAChR complexes), α6β4*, α7, and probably one or more heteromeric subtypes that contain β2 subunits (Hone *et al.* 2012a; Genzen *et al.* 2001; Rau *et al.* 2005), but the role that each of these receptor subtypes play in the detection of painful stimuli and other sensory functions is mostly unknown. Adrenal chromaffin cells, by contrast, may express a more restricted number of subtypes, but have been shown to modify subtype expression patterns under stressful conditions such as prolonged exposure to cold or neuropathic pain (Arribas-Blazquez *et al.* 2019; Colomer *et al.* 2010). Recently, we

showed that human chromaffin cells express mostly α3β4* in addition to α7 nAChRs (Hone *et al.* 2015; Perez-Alvarez *et al.* 2012). Bovine adrenal chromaffin cells have been investigated using selective agonists and positive allosteric modulators (PAMs) of α7 nAChRs (del Barrio *et al.* 2011), but have not been examined using highly selective ligands of other nAChR subtypes. Likewise, very little pharmacological information is available using subtype-specific ligands for rodent adrenal chromaffin cells. Data from functional studies of rat chromaffin cells comes from a single report (Di Angelantonio *et al.* 2003). Furthermore, a quantitative molecular examination of the potential subunits expressed by rat chromaffin cells is also lacking.

Here we report the molecular analysis of the nAChR subunit mRNA transcripts present in rat adrenal medulla by quantitative real-time PCR (qPCR), and the pharmacological characterization of the functionally expressed nAChR subtypes formed from the subunits derived from the identified mRNAs. Using the novel α-conopeptide PeIA-5469, that targets α3β2-containing nAChRs, TxID, a selective antagonist of α3β4-containing nAChRs, and PAMs for α4β2, α4β4, and α7 nAChRs, our results demonstrate that cultured adrenal chromaffin cells from rat express two main heteromeric subtypes namely α3β2β4 and α3β4 nAChRs. These subtypes are expressed by two populations of chromaffin cells: those that express α3β4 and those that express both α3β2β4 and α3β4 subtypes. In addition, functional α7 nAChRs, but not α4-containing subtypes, were found in most cells. The results of these studies identify for the first time the presence of the α3β2β4* subtype as well as functional α7 nAChRs in rat adrenal chromaffin cells.

MATERIALS AND METHODS

Acetylcholine (ACh) chloride (Cat.No. 2809, (year 2019)), PNU120596 (Cat.No. 2498, (year 2019)), and PNU282987 (Cat.No. 2303, (year 2019)) were purchased from Tocris Bioscience (Minneapolis, MN, USA). NS206 was synthesized as previously described (Olsen *et al.* 2013). Sodium chloride (Cat.No. S7653, (year, 2019)), potassium chloride (Cat.No. P9333, (year, 2019)), potassium glutamate (Cat.No. G1149, (year, 2019)), calcium chloride dihydrate (Cat.No. C5080, (year, 2019)), magnesium chloride hexahydrate (Cat.No. M2670, (year, 2019)), dimethylsulfoxide (DMSO) (Cat.No. D8418, (year, 2019)), amphotericin-B (Cat.No. A4888, (year, 2018)), and (4-(2-hydroxyethyl)-1-piperazineethanesulfonic acid) (HEPES) (Cat.No. H3375, (year, 2019)) were purchased from Sigma Aldrich (St. Louis, MO, USA).

Peptide synthesis

Solid-phase Fmoc peptide chemistry and an AAPPTec Apex 396 automated peptide synthesizer (Louisville, KY, USA) were used to synthesize peptides as previously described (Hone *et al.* 2019). Verification of the peptide masses was accomplished by matrix-assisted laser desorption/ionization time-of-flight mass spectrometry at the University of Utah Peptide Synthesis Core facility. The calculated $[MH]^{+1}$ masses of PeIA-5469 and PeIA-5441 are 1777.71 Da and 1758.67 Da and the observed masses were 1777.82 Da and 1758.71 Da, respectively. Peptides will be shared with the research community upon reasonable request.

Two-electrode voltage clamp electrophysiology of *Xenopus laevis* oocytes

Protocols (No. 17–07020) for obtaining oocytes from *X. laevis* frogs were approved by the University of Utah's Institutional Animal Care and Use Committee. Frogs were purchased from Xenopus1 (Dexter, MI, USA) and maintained by university personnel in an AAALAC accredited facility in The School of Biological Sciences at the University of Utah. Oocytes were obtained from frogs that had been anesthetized using 0.4 % wt/vol Tricaine-S (Thermo Fisher Scientific, Waltham, MA, USA); after removal of the ovarian lobes, the frogs were sacrificed. Detailed methods for conducting electrophysiological experiments of nAChRs heterologously expressed in *X. laevis* oocytes have been described previously (Hone *et al.* 2019). Briefly, stage IV-V oocytes were injected at a 1:1 ratio with cRNA encoding cloned rat nAChR subunits α3, α4, α6/α3, α7, α9, α10, β2, β3, or β4 and used 1–5 days after injection. The clones for α3, α4, and α7 subunits were provided by S. Heinemann (Salk Institute, La Jolla, CA, USA), for β2, β3 and β4 by C. Luetje (University of Miami, Miami, FL, USA), and A.B. Elgoyhen (Universidad de Buenos Aires, Buenos Aires, Argentina) provided the α9 and α10 subunits. Construction of the α6/α3 chimera has been described previously (McIntosh *et al.* 2004). The oocytes were clamped at a holding potential of −70 mV and continuously gravity-perfused with frog saline buffered with 5 mM HEPES, pH 7.4. The concentrations of ACh used were 100 μM for β2-containing subtypes and 300 μM for all others and were applied at 60 sec intervals for one second. To assess conopeptides for their ability to inhibit ACh responses, a concentration that produced very little to no inhibition was initially used followed by progressively higher concentrations until complete inhibition was achieved. Conopeptides assessed in this manner were perfusion applied to the oocyte. For conopeptides that showed very little ability to inhibit ACh responses, a single concentration of 10 μM was applied in a static bath for five min.

qPCR of rat adrenal medulla

Protocols (No. 14–08002) for obtaining tissue from rats were approved by the University of Utah's Institutional Animal Care and Use Committee. Male Sprague-Dawley (RRID:RGD_5508397) rats age 30–60 days were obtained from Charles River Laboratories (Wilmington, MA, USA) and housed two per cage in an enriched environment and provided access to food and water *ad libitum*. Three male rats were used to obtain adrenal and pituitary glands for qPCR analysis. Rats were sacrificed with CO_2 and the glands removed and placed in Hank's Balanced Salt Solution (HBSS) (Cat.No. 14175079, (year 2019); Thermo Fisher Scientific, Waltham MA, USA)) buffered with 10 mM HEPES, pH 7.4. The glands from each animal were dissected out and placed separately by animal and by tissue in a 1.5 ml RNAse free Eppendorf tube on dry ice. The mRNA was subsequently isolated using a Qiagen RNeasy Mini Kit (Cat.No. 74104, (year 2018); Qiagen, Valencia, CA, USA)). All mRNA samples were treated with DNase to remove residual genomic DNA. Quantity and purity of the mRNA were determined using an Epoch spectrophotometer (Biotek, Winooski, VT, USA). cDNA was transcribed from one μg of mRNA using Applied Biosystems' (Waltham, MA, USA) High Capacity cDNA Reverse Transcription Kit (Cat.No. 4368813, (year 2018)). TaqMan hydrolysis probes for α2 (Cat.No. Rn00591542_m1, (year 2018)), α3 (Cat.No. Rn00583820_m1, (year 2018)), α4 (Cat.No. Rn00577436_m1, (year 2018)), α5 (Cat.No. Rn00567155_m1, (year 2018)), α6 (Cat.No. Rn00589325_m1, (year 2018)), α7 (Cat.No. Rn00563223_m1, (year 2018)), α9 (Cat.No. Rn01413370_m1, (year 2018)), α10

(Cat.No. Rn00575309_m1, (year 2018)), β2 (Cat.No. Rn00570733_m1, (year 2018)), β3 (Cat.No. Rn00592317_m1, (year 2018)), β4 (Cat.No. Rn00583822_m1, (year 2018)), GAPDH (Cat.No. Rn01775763_g1, (year 2018)), and actin (Cat.No. Rn00667869_m1, (year 2018)) mRNAs as well as the Taqman qPCR Master Mix (Cat.No. 4304437, (year 2018)) were obtained from Applied Biosystems. Fifty ng of cDNA, determined from mRNA quantities, were used for each reaction, and all reactions were run in triplicate. The PCR was carried out using a Bio-Rad CFX98 Touch Real-Time PCR Detection System (Bio-Rad, Hercules, CA, USA) for 40 cycles. Quantitative comparisons of the relative amounts of nAChR subunit mRNAs were determined by normalizing the C_t values to the geometric mean values for actin and GAPDH and the comparative ΔC_t method (Livak & Schmittgen 2001). Comparisons of nicotinic subunit mRNAs between tissues were performed using the $\Delta\Delta C_t$ method. A single group of animals was used and no blinding was performed during experimentation or data analysis.

Adrenal chromaffin cell culture

Protocols (No. 14–08002) for obtaining adrenal glands from rats were approved by the University of Utah's Institutional Animal Care and Use Committee and by the Committee for Research and Ethics of the Universidad Autónoma de Madrid (No. ES-280790000097). Adrenal glands were acquired from male Sprague-Dawley rats age 30–60 days that had been sacrificed using CO_2 or by decapitation. For each culture, the glands of two rats were used for a total of 14 cultures. The adrenal medulla were separated from the adrenal cortex and cut into small pieces using fine iridectomy scissors then transferred to a 1.5 ml tube containing HBSS and 0.25% wt/vol trypsin (Cat.No. 15090046, (year 2019); Thermo Fisher Scientific, Waltham MA, USA)). The medullary pieces were incubated for 30 min at 37 °C and then the solution was aspirated and replaced with HBSS containing 0.1 mg/ml collagenase A (Cat.No. 11088793001 (year 2019); Sigma Aldrich)) and incubated for 30 min at 37 °C. Subsequently, the medullary pieces were triturated with a glass Pasteur pipette with a tip that has been fire polished such that the diameter was approximately half the original size. Once a single cell suspension was obtained, the cells were passed through a 40 μM cell strainer and diluted with 9 ml of HBSS. The cells suspension was centrifuged for 3 min at 200 × g, the solution aspirated, and the cells re-suspended in 500 μl of cell culture medium consisting of Dulbecco's Modified Eagle's Medium (Cat.No. 11960044 (year 2019); Thermo Fisher Scientific)) containing 10% heat-inactivated fetal bovine serum (Cat.No. 10437010, (year 2019); Thermo Fisher Scientific)), 100 μg/ml of streptomycin, 100 U/ml penicillin (Cat.No. 15140122, (year 2019); Thermo Fisher Scientific)), and 100 μM Glutamax (Cat.No. 35050061, (year 2019); Thermo Fisher Scientific)). One-hundred μL of the cell suspension were pipetted onto 15 mm glass coverslips (Cat.No. 67–0703, (year 2019); Warner Instruments, Hamden, CT, USA)) that had previously been treated with 0.1 mg/ml poly-D-lysine (Cat.No. P7280 (year 2019); Sigma Aldrich)). The plated cells were placed in an incubator in an atmosphere of 95% air and 5% CO_2 for 90 min. Thereafter, the wells were flooded with 1 ml of cell culture medium and returned to the incubator.

Whole-cell patch-clamp electrophysiology

Electrophysiology experiments were conducted on chromaffin cells that had been in culture for at least 36 hours and up to four days after the day of isolation. Experiments were

initiated by placing a coverslip containing the cells in an electrophysiology chamber and continuously perfusing them with extracellular saline solution composed of 145 mM NaCl, 5 mM KCl, 2 mM $CaCl_2$, 1 mM $MgCl_2$, and 10 mM HEPES, pH 7.4, observed osmolarity was 310 mOsM. The solutions were controlled by a custom perfusion system. The valve box consisted of five solenoid valves (Cat.No LFAA1200218H; (year 2016), Lee Valve Company, Westbrook, CT, USA, purchased from Radwell International, Inc., Lumberton, NJ, USA)) connected to a CoolDrive Valve Driver (Cat.No. 161D5X12 (year 2016); NResearch, West Caldwell, NJ, USA)) interfaced with a computer using a National Instruments (Austin, TX, USA) 6009 DAQ and controlled using a custom virtual instrument program written in National Instruments LabView 2015 (RRID:SCR_014325). These valves were used for perfusion of extracellular solution. The valve box also contained two additional valves individually connected to an Axon Instruments 1550A digitizer (Axon Instruments, San Jose, CA, USA) via CoolDrive One Valve Drivers (Cat.No. 161D1X250, (year 2019); NResearch) and were controlled by PClamp 10.2 software (RRID:SCR_011323; Axon Instruments). These valves were used for agonist applications. The tubing used for the five extracellular solution and two agonist perfusion lines were made from Teflon tubing with an outer diameter of 1.58 mm and an inner diameter of 0.8 mm and were connected to a custom solution distributor. This distributor was constructed from 200 µl plastic pipette tips and seven polyethylene tubes with outer diameters of 1.09 mm and inner diameters of 0.15 mm. These tubes coalesced to a single outlet tube also constructed from a 200 µl pipette tip and a 3.5 mm long tube of the same diameter polyethylene tubing. The flow rate of this system was approximately 850 µl/min and gravity fed. Experiments performed to assess the potency of TxID for inhibition of ACh-evoked currents in chromaffin cells were conducted under similar conditions but with a perfusion control system described elsewhere (Hone *et al.* 2015).

Electrodes were constructed from thick-walled borosilicate glass with an outer diameter of 1.5 mm (Cat.No. PG52151–4, (year 2019); World Precision Inc., Sarasota, FL, USA)) and pulled using a Sutter P97 puller (Sutter Instruments, Novato, CA, USA). The resistances of the electrodes were between 2–4 MΩ when filled with an internal electrode solution composed of 145 mM K-glutamate, 10 mM NaCl, 1 mM, $MgCl_2$, and 10 mM HEPES, pH 7.3, observed osmolarity was 310 mOsM. The tips of the electrodes were filled by dipping them in internal electrode solution then backfilling them with the same solution containing 0.5 mg/ml amphotericin-B. The amphotericin-B stock solution (50 mg/ml) was prepared in 100% DMSO. Ten µl of this solution was added to 1 ml internal electrode solution and briefly ultra-sonicated prior to filling each electrode.

After obtaining a GΩ seal, the membrane resistance of the cells was monitored and experiments were begun after the access resistance (R_a) had decreased to < 20 MΩ; values of R_a were usually between 6–15 MΩ and were compensated electronically up to 80%. The cells were continuously perfused with extracellular solution and stimulated once every 90 sec with 500 ms pulses of ACh (300 µM). The ACh-evoked currents were obtained at a holding potential of −70 mV, digitized at 10 kHz and filtered at 1 kHz using an Axon Instruments Multiclamp 700B and a Digidata 1550A (Molecular Devices, San Jose, CA, USA). Experiments conducted to assess the potency of TxID for inhibition of ACh-evoked currents in chromaffin cells were conducted under similar conditions, but in these

experiments the currents evoked by ACh (200 ms pulses) were obtained at a holding potential of −80 mV, digitized at 10 kHz and filtered at 1 kHz using an EPC 10 amplifier controlled by FITMASTER software (RRID:SCR_016233; HEKA Electronik GmbH, Lambrecht, Germany). After stable current amplitudes were observed, the extracellular solution was switched to one containing the ligand of interest, and the current responses monitored for changes in amplitudes. Changes in current amplitudes were normalized to the average of at least three responses in the absence of ligand. A single group of animals was used and no blinding was performed during experimentation or data analysis.

Drug solution preparation

Acetylcholine chloride was prepared as a 1 M stock solution in distilled water. To overcome the poor solubility of PNU282987, PNU120596, and NS206 in aqueous solutions, 100 mM stock solutions were prepared in 100% DMSO. To prepare working solutions, extracellular solution was heated to 50 °C and the compounds added to obtain final concentrations of 30 μM PNU282987, 3 μM PNU120596, or 10 μM NS206. The solutions were allowed to cool to room temperature overnight and subsequently filtered through a 0.22 μm filter. All α-Ctxs and their derivatives were prepared as 100 μM stock solutions in extracellular solution.

Statistical analysis

To compare differences in relative gene expression in qPCR experiments, an analysis of variance (ANOVA) with a Holm-Šídák post hoc test for significance was used; the data were analyzed for normality using a Shapiro-Wilk test. For assessing the potencies of α-Ctxs and their analogs, data were collected from a minimum of four oocytes unless indicated otherwise and from four adrenal chromaffin cells for each IC_{50} determination. The data were analyzed using the Hill equation and the IC_{50} values presented with the corresponding 95% confidence intervals for evaluation of the precision of the IC_{50} estimate. A Student's *t*-test was used to analyze the effects of single concentrations of α-Ctxs and other ligands on agonist-evoked currents in chromaffin cells. The data were analyzed for normality using a Shapiro-Wilk test or a D'Agostino-Pearson omnibus test. For data sets that were determined not to be normally distributed, a Wilcoxon Signed Rank test was used. Significance was determined at the 95% level in all analyses; ns, not significant, $p>0.05$; *$p\leq0.05$; **$p\leq0.01$; ***$p\leq0.001$ and ****$p\leq0.0001$. Data were not assessed for outliers and no data points were excluded from analysis. For all data sets, the '±' values and all error bars indicate the SD to show the variance of the data. Data analyses were performed using Graph Pad Prism 6 (RRID:SCR_002798; GraphPad, La Jolla, CA, USA) or SigmaPlot 14.0.3 (RRID:SCR_003210; Systat Software, San Jose, CA, USA).

RESULTS

qPCR of rat adrenal medulla reveals the presence of mRNAs for multiple nAChR subunits

We began our examination of the nAChRs expressed by rat adrenal chromaffin cells by conducting qPCR experiments of whole rat adrenal medulla to assay for the presence of mRNAs for α2-α7, α9, α10, and β2-β4 subunits. As a tissue for comparison, we also assessed the pituitary gland which forms part of the hypothalamic-pituitary-adrenocortico (HPA) axis and plays an intimate role in chromaffin cell physiology and the response to

stress. In the adrenal medulla, mRNA transcripts for α3, α5, α7, β2 and β4 subunits were found in relative high abundance ($C_t \leq 30$), whereas lower levels ($C_t < 35$ and > 30) were found for α4 subunits (Fig. 1A; Table 1). Transcripts for all other subunits were >20,000-fold less abundant than those of α3 (Fig. 1C; Table 1). By contrast, the most abundant transcripts found in the pituitary gland were for α4, α7, α9, β2 and β4 subunits ($C_t \leq 30$) with lower levels found for and α2, α3, α5, and α10, ($C_t < 35$ and > 30) (Fig. 1C and D). The three most abundant mRNAs in the adrenal medulla, α3, α7, and β4, were significantly higher than those in the pituitary whereas transcripts for β2 subunits were expressed in equal amount in both tissues (Fig. 1E; Table 1). These results suggest that rat adrenal chromaffin cells potentially express several heteromeric nAChRs containing β2 and/or β4 subunits and may include α3β2, α3β4, α4β2, α4β4. The relatively high levels of α7 transcripts present in adrenal medulla also suggest that receptors containing α7 subunits are probably expressed as well.

Synthesis and characterization of a highly selective α-conopeptide ligand for α3β2 nAChRs

Current ligands that inhibit α3β2 nAChRs often interact with the closely related α3β4 subtype or have very slow binding kinetics that make their use challenging in functional *in vitro* studies. In order to develop a ligand that is highly selective for α3β2 over α3β4 nAChRs and that displays favorable binding kinetics, we assessed the potencies of 16 PeIA analogs on α3β4 nAChRs expressed in *X. laevis* oocytes and compared the results to data previously obtained for α3β2 nAChRs (Hone *et al.* 2019). These analogs contain select amino acid substitutions of Ser^9, Val^{10}, Asn^{11}, or Leu^{15}. Several noteworthy observations were made with respect to the activity of these analogs on α3β4 nAChRs. First, analogs [Asp^9]PeIA and [Arg^9]PeIA showed substantially reduced potency relative to the native peptide (Fig. 2A; Table 2). By contrast, [Tyr^9]PeIA showed increased potency (Fig. 2A; Table 2). Analogs with substitutions of Val^{10} showed either no change or only small changes in potency relative to native PeIA (Fig. 2B; Table 2). We have previously shown that substitution of Asn^{11} with negatively charged non-natural amino acids can alter the interaction between PeIA and α3β2 nAChRs (Hone *et al.* 2019). In the case of α3β4 nAChRs, substitution of Asn^{11} with α-aminosuberic acid (Asu) resulted in enhanced potency whereas α-aminoadipic acid (Adi) reduced the potency of PeIA (Fig. 2C; Table 2). Substitution of Asn^{11} with α-aminopimelic acid (Api) had no effect on the potency of PeIA for α3β4 nAChRs. Lastly, we determined the effects of substitution of Leu^{15} with Ile, Val, Ala, and norleucine (Nle). The amino acids Ile and Val enhanced PeIA potency for α3β4 nAChRs whereas Ala and Nle had no effect (Fig. 2D; Table 2).

The structure-activity analysis of PeIA on α3β4 nAChRs suggested that several amino acids might selectively decrease potency for α3β4 nAChRs while preserving potency on the α3β2 subtype. Therefore, we synthesized two peptides incorporating Arg or His, Ile, Api, and Nle in the 9th, 10th, 11th, and 15th positions, respectively. The sequences of the resulting peptides are GCCSHPACRI(Api)HPE(Nle)C (PeIA-5469) and GCCSHPACHI(Api)HPE(Nle)C (PeIA-5441). The peptides were tested on a panel of nAChR subtypes to determine their potencies and selectively profiles. Both peptides showed high potency ($IC_{50} < 10$ nM) for α3β2 nAChRs (Fig. 3A and B). Importantly, PeIA-5469

and PeIA-5441 were 1,175- fold and 198-fold selective for α3β2 over α3β4 nAChRs. Both peptides were also substantially less potent on α4β2 and α4β4 nAChRs. In fact, PeIA-5469 was essentially inactive (IC_{50} > 10 μM) on both subtypes. Next, we assessed the binding kinetics of PeIA-5469 and PeIA-5441 on α3β2 nAChRs. Oocytes expressing α3β2 nAChRs were sequentially perfused with PeIA-5469 followed by PeIA-5441 to assess the rate at which the peptides inhibited the ACh responses as well as dissociation rate of the peptides from the receptors (Fig. 4A). Despite the high sequence similarity between the two peptides, PeIA-5469, with Arg^9, displayed significantly faster kinetics. Although the inhibition rates were similar at the concentration used (100 nM) (Fig. 4B), analysis of the recovery rates determined that PeIA-5469 dissociated from the receptors at a ~28-fold faster rate (Fig. 4C). Full recovery of the ACh responses after exposure to PeIA-5469 occurred in about 5 min whereas after a 20 min wash, the responses had only recovered to 50 ± 10% (n=4) after exposure to PeIA-5441.

PeIA-5469 and TxID identify α3β2β4 and α3β4 as the main heteromeric nAChR subtypes expressed by rat adrenal chromaffin cells

The synthesis of PeIA-5469 provided a valuable tool with which to assess adrenal chromaffin cells for the expression of α3β2 nAChRs. Patch-clamp electrophysiology was used to pharmacologically assess the sensitivity of ACh-evoked responses to inhibition by nAChR antagonists. The cells were voltage-clamped at −70 mV and stimulated with ACh (300 μM). The nAChR subtypes mediating the ACh-evoked currents were determined by perfusing the cells with subtype-selective antagonists. We found that a majority (60%) of the cells displayed ACh-evoked currents that were insensitive to PeIA-5469 (101 ± 3% of controls, n=10; Fig. 5A and D) but had currents that could be nearly completely inhibited by the α3β4 antagonist TxID (3 ± 1%, n=10). However, a subset of cells (40%) had currents that were inhibited in the presence of PeIA-5469 (71 ± 7% of controls; −2073 ± 805 pA vs −1500 ± 705 pA, respectively; ****$p \leq 0.0001$, n=7; Fig. 5B and D). In this same set of cells, and after washout of PeIA-5469, subsequent exposure to TxID inhibited the ACh-evoked currents to 2 ± 2% (n=7) of control values. These results indicate that in this minority population, chromaffin cells express a nAChR subtype that is sensitive to inhibition by both α3β2 and α3β4 antagonists. Although the α7 antagonist [V11L,V16D]ArIB was included in all perfusion solutions, control experiments were performed by perfusing the cells with TxID without prior exposure to PeIA-5469 to ensure that the effects observed by PeIA-5469 were due to inhibition of α3β2 nAChRs and not of potential α7-mediated responses. In this case, TxID inhibited the responses to 3 ± 1% (n=14) of control values (Fig. 5C). No significant differences were found with respect to the level of inhibition produced by perfusion with TxID only compared to that produced by TxID after perfusion with PeIA-5469. (Fig. 5D). Additionally, we also assessed the potency of TxID for inhibition of α3β4 nAChRs expressed in chromaffin cells and compared the results to the IC_{50} value previously reported for rat α3β4 nAChRs expressed in *X. laevis* oocyte (Luo *et al.* 2013). An IC_{50} value of 7.0 (6.3–7.8) nM (Fig. 6) was obtained and was similar to the value (13 nM) obtained for heterologously expressed rat α3β4 nAChRs.

Rat adrenal chromaffin cells lack α4β2 and α4β4 nAChRs

qPCR results suggested that nAChRs containing the α4 subunit may also be expressed by chromaffin cells (Fig. 1). However, expression levels of such receptors are likely low relative to α3β4 nAChRs as TxID inhibited ~97% of the ACh-evoked currents in all cells in which this antagonist was applied (n=35). We used the PAM NS206 that increases agonist-evoked current amplitudes mediated by α4β2 and α4β4 nAChRs (Olsen *et al.* 2013) to determine if these subtypes were expressed by chromaffin cells. The cells were perfused first with TxID, to inhibit α3β4 nAChRs, then with NS206 in the presence of TxID. Similar to the results presented in Figure 4, TxID almost completely inhibited the ACh-evoked currents and no increase in the residual current was observed upon exposure to NS206 (Fig. 7A). In fact, currents in the presence of TxID and NS206 were smaller than those in the presence of TxID alone (Fig. 7B). These results suggest that there are few α4-containing nAChRs expressed by rat chromaffin cells under the conditions used in this study.

Rat adrenal chromaffin cells express functional α7 nAChRs

A previous report indicated that rat adrenal chromaffin cells lack functional α7 nAChRs (Di Angelantonio *et al.* 2003). The discovery of selective agonists and PAMs of α7 nAChRs has facilitated the identification of α7 nAChRs in cells where α7-mediated responses have been difficult to detect with agonists alone (Perez-Alvarez *et al.* 2012; del Barrio *et al.* 2011; Smith *et al.* 2013; Chatzidaki *et al.* 2015). PNU282987 is an α7-selective agonist (Bodnar *et al.* 2005) and PNU120596 is a PAM that relieves receptor desensitization thereby increasing response amplitude and duration (Hurst *et al.* 2005). To determine if rat chromaffin cells express functional α7 nAChRs, we stimulated the cells first with 500 ms pulses of ACh followed by pulses of PNU282987 of the same duration, then the perfusion solution was changed from normal saline to one containing PNU120596. In 18/28 cells, PNU282987 evoked relatively small amplitude currents compared to those evoked by ACh in the same cells (Fig. 8A and B). Subsequent stimulation of the cells with PNU282987 in the presence of PNU120596 evoked detectable currents from 24/28 cells including from six cells that initially showed no response to PNU282987. These PNU120596-modulated currents were sensitive to inhibition by the α7-selective peptide [V11L,V16D]ArIB (Fig. 8A and B). In 4/28 cells, no response was observed upon stimulation of the cells with the PNU282987 in the presence of the PAM (Fig. 8C). To assess if repeated stimulation of the cells with ACh prior to stimulation with PNU282987 resulted in undetectable α7-mediated responses, we conducted additional experiments where the order of agonist application was reversed. In these experiments, the cells were stimulated with PNU282987 first followed by ACh. Under these conditions, all of the cells tested responded to PNU282987 (Fig. 9A–C; n=7). Next we assessed whether α7 subunit-containing nAChRs were present but not sensitive to PNU282987 by stimulating the cells with ACh and then exposing them to [V11L,V16D]ArIB alone followed by TxID. The current amplitudes in the presence of [V11L,V16D]ArIB were no different than control values but were nearly completely inhibited in the presence of TxID (Fig. 9D and E). These results indicate that >97% of the whole-cell ACh-evoked currents in rat adrenal chromaffin cells are mediated by α3β2β4 and α3β4 nAChRs, and that the α7 subtype accounts for only a small proportion of the response.

DISCUSSION

nAChRs have been investigated for some time as potential therapeutic targets, but very little success has been achieved because often times the developed compounds target multiple nAChR subtypes producing unwanted side effects. For example, varenicline is a nicotine replacement therapeutic whose mechanism of action in reducing the consumption of nicotine is believed to be *via* partial activation of α4β2* nAChRs in the brain (Rollema *et al.* 2010; Coe *et al.* 2005). Unfortunately, varenicline's use has been associated with cardiovascular side effects (Singh *et al.* 2011; Gershon *et al.* 2018; Harrison-Woolrych *et al.* 2012), possibly because of the activation of non α4β2 subtypes including α3β2 and α3β4 (Stokes & Papke 2012; Mihalak *et al.* 2006). Indeed, it has been shown that therapeutic concentrations of varenicline alter the excitability of human adrenal chromaffin cells in the presence of nicotine (Hone *et al.* 2017). The consumption of nicotine itself is also associated with altered cardiovascular activity which may result from the activation of chromaffin cell expressed nAChRs as it has been shown to evoke catecholamine release from these cells (Mizobe & Livett 1983). Thus, it is important to determine the nAChR subtypes expressed by chromaffin cells and to investigate the effects that potential therapeutic compounds have on adrenal chromaffin cell activity.

Despite the widespread use of rat adrenal chromaffin cells in neuroscience, a detailed analysis of the nAChRs expressed by these cells has not been reported. Here we have examined the nAChRs expressed by rat chromaffin cells using molecular biology and pharmacology. qPCR experiments of rat adrenal medulla suggested that nAChRs composed of α3, α4, α5, α7, β2 or β4 subunits may be expressed by chromaffin cells (Fig. 1). The potential expression of multiple nAChR subtypes by adrenal chromaffin cells, and other cell types, requires highly selective ligands that can distinguish among the various subtypes (Giribaldi & Dutertre 2018). α-Conotoxin TxID is a potent antagonist of α3β4 nAChRs and is essentially devoid of activity on the other potential subtypes expressed by chromaffin cells (Luo *et al.* 2013). The α7 subtype can be distinguished from all other nAChRs using the α-Ctx ArIB analog [V11L,V16D]ArIB (Whiteaker *et al.* 2007). A summary of the previously reported IC_{50} values of TxID and [V11L,V16D]ArIB for various rat nAChRs is presented in Table 4.

Recently, we described a novel set of PeIA analogs that are highly selective for α3β2 nAChRs (Hone *et al.* 2019). One analog in particular, PeIA-5355, was >1,300-fold selective for α3β2 over α3β4 but also inhibited α6/α3β2β3 nAChRs. A related analog, PeIA-5466, discriminated well between α3β2 and α6/α3β2β3 nAChRs but had slightly less ability to distinguish between α3β2 and α3β4 receptors (IC_{50} ratio 292) (Hone *et al.* 2019). These PeIA analogs display very slow dissociation kinetics for α3β2 nAChRs with full response recovery requiring >25 min. Although slow ligand dissociation kinetics can be useful characteristics in some experimental situations, under patch-clamp and other *in vitro* conditions where it may be desirable and advantageous to apply several ligands to a single cell, slow ligand kinetics can be problematic. Therefore, in order to characterize the potential α3-containing subtypes expressed by rat adrenal chromaffin cells, we sought to develop an α3β2-selective ligand with rapid kinetics that would allow the application of multiple subtype-selective ligands to the same cell under study.

Previous structure-activity relationship studies identified position nine in the sequence of PeIA as playing a critical role in binding to α3 and α6 subtypes. For example, substitution of Ser^9 with His increased PeIA potency for rat α3β2, α6/α3β2β3, α3β4, and α6/α3β4 subtypes and substantially slowed the on- and off-rate kinetics (Hone *et al.* 2012b). By contrast, substitution of Ser^9 with Arg selectively increased potency for α3β2 and α6/α3β2β3 but significantly decreased potency for α6β4 nAChRs (Hone *et al.* 2013). Similarly, we found that [Arg^9]PeIA also showed substantially reduced activity compared to native PeIA when tested on α3β4 nAChRs (Fig. 2A; Table 2). Additional structure-activity relationship data were obtained for the α3β4 subtype by testing analogs of PeIA with substitutions of Val^{10}, Asn^{11}, and Leu^{15}. Substitution of Val^{10} with Ile reduced PeIA potency for α3β4 nAChRs (Fig. 2B; Table 2). Although substitutions of Asn^{11} and Leu^{15} had very little impact on PeIA potency for α3β4 nAChRs (Fig. 2A, C, and D; Table 2), N11Api and L15Nle substitutions have been shown to be favorable for reducing activity on other non α3β2 subtypes (Hone *et al.* 2019). Informed by these data, we synthesized PeIA-5469 that incorporated Arg^9, Ile^{10}, Api^{11}, and Nle^{15} (Fig 3A). For comparison, we also synthesized PeIA-5441 that is identical in sequence to PeIA-5469 with the exception of His^9 (Fig 3B). qPCR data indicated that α3β2, α3β4, α4β2, and α4β4 were the most likely heteromeric nAChRs expressed by rat adrenal chromaffin cells and when tested on these nAChR subtypes heterologously expressed in oocytes, PeIA-5469 showed high potency (IC_{50} 8.6 nM) for α3β2 and was >1,000-fold less potent on other tested subtypes (Fig. 3A). Whereas PeIA-5469 is much more potent on α3β2 than α3β4, α4β2, and α4β4 the margins of selectivity were narrower for PeIA-5441 (Fig. 3B). Furthermore, the off-rate kinetics were substantially different between the two peptides (Fig. 4). The responses to ACh in oocytes expressing α3β2 nAChRs recovered >20-fold more slowly after exposure to PeIA-5441 than PeIA-5469 (Fig. 4C). Importantly, the $t_{1/2}$ for recovery of the responses after exposure to PeIA-5469 was < 60 sec. PeIA-5469 therefore possesses the desired qualities of being highly selective for α3β2 nAChRs and displays rapid kinetics.

The relative abundance of mRNA for the β2 subunit in rat adrenal medulla suggested that receptors containing this subunit may be expressed by chromaffin cells (Fig. 1). The most likely candidate for combining with β2 subunits to form heteropentameric receptors is probably α3 based on the abundance of mRNA for α3 subunits. However, mRNA for the α4 subunit was also detected albeit at significantly lower levels compared to those for α3 and therefore it was possible that α4β2 nAChRs were also expressed. The development of PeIA-5469 allowed us to assess chromaffin cells for the expression of α3β2 nAChRs and to pharmacologically distinguish this subtype from α3β4, α4β2, and α4β4 subtypes. Under electrophysiological conditions, we stimulated chromaffin cells with ACh and then perfused them with PeIA-5469 to assay for the presence of α3β2 nAChRs. In some cells, exposure to PeIA-5469 had little effect on the ACh-evoked current amplitudes and, instead, TxID inhibited the responses in these same cells by ~97% (Fig. 5A and D). However, in a subset of cells a significant reduction of ~30% of the ACh-evoked currents by PeIA-5469 was observed (Fig. 5B and D). Following washout of PeIA-5469, these same cells were then exposed to TxID and, interestingly, the current amplitudes were reduced to about 2% of control values. Together, these data suggest the presence of a nAChR with both α3-β2 and α3-β4 ligand-binding interfaces. Such a receptor would have a composition of α3β2α3β4

with an unknown subunit in the 5th position. Furthermore, the fact that the ACh-evoked currents in some cells could be inhibited by PeIA-5469 and by TxID indicates that a subset of cells expresses two types of α3-containing receptors. In one population, comprising 60%, the majority of the nAChRs appear to be α3β4 whereas in the minority population (40%), the cells express both α3β4 and α3β2β4 subtypes.

We have previously shown that α3β4* nAChRs natively expressed by human adrenal chromaffin cells and heterologously expressed in *X. laevis* oocytes show very similar sensitivities to TxID. To ensure that this was also the case for rat α3β4 nAChRs, we determined the IC_{50} value for rat adrenal chromaffin cell-expressed receptors and found that the IC_{50} value was less than 2-fold different (Fig. 5) from the value previously obtained for rat α3β4 nAChRs expressed in oocytes (Luo *et al.* 2013). The similarities between these IC_{50} values indicate that TxID retains high potency and selectivity for native rat α3β4 nAChRs.

Native α3β2β4 nAChRs have been reported in several classes of neurons in the peripheral nervous system (Mao *et al.* 2006; David *et al.* 2010; Bibevski *et al.* 2000) but not previously in adrenal chromaffin cells. In mouse superior cervical ganglion, neurons express three distinct α3-containing nAChRs that include α3β4, α3β4α5, and α3β2β4 and display differential sensitivities to agonists and differ in their biophysical properties including desensitization rates and single-channel conductance (Ciuraszkiewicz *et al.* 2013; David *et al.* 2010). In general, the α3β2 subtype is more sensitive to ACh and desensitizes more quickly than does the α3β4 subtype. In the context of catecholamine release from adrenal chromaffin cells, the presence of two nAChR subtypes with potentially different sensitivities to ACh and biophysical properties may serve to modulate exocytosis under particular physiological conditions (homeostatic release vs. release under stressful conditions, for example). The presence of substantial levels of mRNA for α5 subunits also suggests that rat chromaffin cells may also express α3β4 receptors that contain this subunit giving rise to α3β4α5 or α3β2β4α5 nAChRs. Unfortunately, at the present time there are no known ligands that selectively target subtypes containing the α5 subunit.

Although [V11L,V16D]ArIB was included in all perfusion solutions, an alternative possibility with respect to the inhibition observed by PeIA-5469 was that this new α3β2 antagonist inhibited residual α7 nAChR mediated responses. We assessed this possibility by perfusing cells with TxID that had not been previously exposed to PeIA-5469 to determine if α7-mediated responses were observed. Under these conditions, the residual currents in the presence of TxID were about 3% of control values (Fig. 5C and D). A statistical analysis revealed that there was no significant difference in the level of inhibition produced by TxID applied singly or after application of PeIA-5469 suggesting that it was unlikely that the response inhibition produced by PeIA-5469 was of α7 nAChRs.

Initial reports that examined the nAChR subtypes expressed by adrenal chromaffin cells suggested through radioligand-binding studies using the α7 antagonist α-bungarotoxin that rodent, bovine, and feline chromaffin cells express α7 nAChRs (Criado *et al.* 1997; El-Hajj *et al.* 2007). More recently, according to immunohistochemical evidence mouse chromaffin cells show prominent expression of α7 nAChRs in a population with a norepinephrine

synthesizing phenotype (Gahring *et al.* 2014), and *in situ* hybridization studies suggest that there is developmental regulation of the α7 gene (CHRNA7) in the adrenal medulla (Broide *et al.* 2019). Nevertheless, functional demonstration of α7 nAChRs in rodent chromaffin cells had not been reported previously, and in fact rat chromaffin cells have been reported to lack functional α7 nAChRs (Di Angelantonio *et al.* 2003).We found through qPCR experiments that rat adrenal medulla contains relatively high levels of α7 subunit mRNA in support of the presence of α7 nAChRs (Fig. 1). The development of highly selective agonists, PAMs, and antagonists of α7 nAChRs has facilitated the identification of natively expressed α7 receptors in numerous cell types from several mammalian species (Perez-Alvarez *et al.* 2012; Hone *et al.* 2012a; Smith *et al.* 2013; del Barrio *et al.* 2011; Kalappa *et al.* 2010). Here we used the antagonist [V11L,V16D]ArIB (Whiteaker *et al.* 2007) in combination with the α7-selective agonist PNU282987 (Hajos *et al.* 2005) and the PAM PNU120596 (Hurst *et al.* 2005) to probe for the expression of functional α7 nAChRs in rat adrenal chromaffin cells. We found that in a little more than half of the cells (18/28), stimulation with PNU282987 evoked relatively small amplitude currents (Fig. 8A and C). Upon exposure to PNU120596, detectable PNU282987-evoked currents were recorded in 24/28 cells (Fig. 8A and B). Only in 4/28 cells did PNU282987 fail to evoke responses in the presence of the PAM (Fig. 8C). Currents evoked by PNU282987 and modulated by PNU120596 were sensitive to inhibition by [V11L,V16D]ArIB (Fig. 8B).

Additional experiments were conducted to determine if the lack of PNU282987-evoked currents in some cells was due to experimental factors, such as repeated stimulation with agonists that can reduce the functionality of nAChRs due to desensitization. To address this concern, we reversed the order of agonist application and stimulated the cells first with PNU282987 followed by ACh. In this case, PNU282987-evoked currents were detected in all seven of the cells subjected to this protocol (Fig. 9A–C). In some cells, the current amplitudes were relatively small (10–20 pA) and therefore it is reasonable to conclude that small α7-mediated responses may have declined during the course of the experiment (Fig. 8). It is likely, then, that the initial experiments underestimated the percentage of cells that would have responded to PNU282987. Regardless, the α7-mediated responses were relatively small compared to those mediated by α3β2β4 and α3β4 subtypes (Fig. 9C–E). Taken together, these data unequivocally demonstrate that rat adrenal chromaffin cells do in fact express functional α7 nAChRs. Nevertheless, most of the α7 nAChRs in these cells appear to be in a state where the probability of channel gating by an agonist is very low. Thus, although rat chromaffin cells express functional α7 nAChRs, it is unclear what role these ligand-gated ion channels play in the physiology of the cells given their profound insensitivity to gating by agonists and small amplitude currents. Functional studies using bovine and human chromaffin cells have demonstrated that under certain experimental conditions, secretion of catecholamines through PNU120596-modulated activation of α7 nAChRs can be achieved (Fuentealba *et al.* 2004; Perez-Alvarez *et al.* 2012; del Barrio *et al.* 2011). High concentrations of choline or PNU282987 alone have also been shown to elicit APs and evoke release in human chromaffin cells (Perez-Alvarez *et al.* 2012). However, studies using physiological concentrations of ACh or choline to assess the contribution of α7 nAChRs to the secretory process have been equivocal (Lopez *et al.* 1998; Broxton *et al.* 1999). Thus, continuing controversy surrounds the functional role of α7 nAChRs in the

secretory processes of adrenal chromaffin cells (Criado 2018; Albillos & McIntosh 2018; Sala *et al.* 2008).

Lastly, qPCR experiments detected mRNA for α4 subunits (Fig. 1) and therefore to assess the cells for the presence of α4-containing nAChRs, we used the PAM NS206 that selectively potentiates responses mediated by α4β2 and α4β4 nAChRs (Olsen *et al.* 2013). The cells were exposed to TxID to inhibit α3β4 and α3β2β4 subtypes and the residual responses were probed for the presence of α4-containing nAChRs by assessing the ACh responses for increased amplitudes upon perfusion with NS206. However, rather than increased amplitudes, we observed further inhibition of the ACh-evoked currents (Fig. 7A). Analysis of the currents in the presence of TxID vs. those in the presence of TxID together with NS206 revealed a significant reduction in amplitudes upon perfusion with NS206 (Fig. 7B). These results suggest that not only are there very few α4-containing nAChRs sensitive to NS206, but that this ligand is probably an antagonist of the α3-containing nAChRs expressed in rat chromaffin cells.

In this report, we describe the development of PeIA-5469, a highly selective antagonist of α3β2 nAChRs that was used to identify for the first time the expression of the α3β2β4 subtype in rat adrenal chromaffin cells. The selectivity profile and favorable binding kinetics of PeIA-5469 allowed us to apply multiple ligands to the same cell to individually characterize the nAChR subtypes expressed by each. The results of these studies show that rat adrenal chromaffin cells express α3β2β4, α3β4, and α7 nAChRs and do not appear to express substantial numbers of α4β2 or α4β4 nAChRs. Adrenal chromaffin cells are widely used to study the release of neurotransmitters and the information obtained by these studies may be useful for future studies examining the contributions of individual subtypes to exocytosis and the roles of chromaffin cells in conditions such as PTSD, neurodegenerative diseases (de Diego & Garcia 2018), inflammation (Kanczkowski *et al.* 2015), and neuropathic pain (Arribas-Blazquez *et al.* 2019).

```
Conflicts of interest:  none
=> if ‘none’, insert “The authors have no conflict of interest to declare.”
=> otherwise insert info unless it is already included
```

Acknowledgements

Funding

Funding for this study was provided by NIH grants GM103801, GM48677, and DA042749 to JMM, a Marie Curie postdoctoral fellowship grant NRHACC from the European Research Council FP7 to AJH, and by the Spanish Ministry of Science and Innovation [Grants BFU2012-30997 and BFU2015-69092] awarded to AA.

Abbreviations

nAChRs	Nicotinic acetylcholine receptors
ACh	acetylcholine
PAM	Positive allosteric modulator
α-Ctx	α-Conotoxin
PACAP	pituitary adenylate cyclase-activating polypeptide
qPCR	Quantitative polymerase chain reaction
HEPES	4-(2-hydroxyethyl)-1-piperazineethanesulfonic acid
DMSO	dimethylsulfoxide
RRDI	Research Resource Identifier

REFERENCES

Albillos A and McIntosh JM (2018) Human nicotinic receptors in chromaffin cells: characterization and pharmacology. Pflugers Arch 470, 21–27. [PubMed: 29058146]

Arribas-Blazquez M, Olivos-Ore LA, Barahona MV et al. (2019) Overexpression of P2X3 and P2X7 Receptors and TRPV1 Channels in Adrenomedullary Chromaffin Cells in a Rat Model of Neuropathic Pain. Int J Mol Sci 20.

Biales B, Dichter M and Tischler A (1976) Electrical excitability of cultured adrenal chromaffin cells. J Physiol 262, 743–753. [PubMed: 1034699]

Bibevski S, Zhou Y, McIntosh JM, Zigmond RE and Dunlap ME (2000) Functional nicotinic acetylcholine receptors that mediate ganglionic transmission in cardiac parasympathetic neurons. J Neurosci 20, 5076–5082. [PubMed: 10864965]

Bodnar AL, Cortes-Burgos LA, Cook KK et al. (2005) Discovery and structure-activity relationship of quinuclidine benzamides as agonists of alpha7 nicotinic acetylcholine receptors. Journal of medicinal chemistry 48, 905–908. [PubMed: 15715459]

Brandt BL, Hagiwara S, Kidokoro Y and Miyazaki S (1976) Action potentials in the rat chromaffin cell and effects of acetylcholine. J Physiol 263, 417–439. [PubMed: 1018274]

Broide RS, Winzer-Serhan UH, Chen Y and Leslie FM (2019) Distribution of alpha7 Nicotinic Acetylcholine Receptor Subunit mRNA in the Developing Mouse. Front Neuroanat 13, 76. [PubMed: 31447654]

Broxton NM, Down JG, Gehrmann J, Alewood PF, Satchell DG and Livett BG (1999) Alpha-conotoxin ImI inhibits the alpha-bungarotoxin-resistant nicotinic response in bovine adrenal chromaffin cells. J Neurochem 72, 1656–1662. [PubMed: 10098874]

Chatzidaki A, Fouillet A, Li J, Dage J, Millar NS, Sher E and Ursu D (2015) Pharmacological Characterisation of Nicotinic Acetylcholine Receptors Expressed in Human iPSC-Derived Neurons. PLoS One 10, e0125116. [PubMed: 25906356]

Ciuraszkiewicz A, Schreibmayer W, Platzer D, Orr-Urtreger A, Scholze P and Huck S (2013) Single-channel properties of alpha3beta4, alpha3beta4alpha5 and alpha3beta4beta2 nicotinic acetylcholine receptors in mice lacking specific nicotinic acetylcholine receptor subunits. J Physiol 591, 3271–3288. [PubMed: 23613527]

Coe JW, Brooks PR, Vetelino MG et al. (2005) Varenicline: an alpha4beta2 nicotinic receptor partial agonist for smoking cessation. Journal of medicinal chemistry 48, 3474–3477. [PubMed: 15887955]

Colomer C, Olivos-Ore LA, Vincent A, McIntosh JM, Artalejo AR and Guerineau NC (2010) Functional characterization of alpha9-containing cholinergic nicotinic receptors in the rat adrenal medulla: implication in stress-induced functional plasticity. J Neurosci 30, 6732–6742. [PubMed: 20463235]

Criado M (2018) Acetylcholine nicotinic receptor subtypes in chromaffin cells. Pflugers Arch 470, 13–20. [PubMed: 28791474]

Criado M, Dominguez del Toro E, Carrasco-Serrano C, Smillie FI, Juiz JM, Viniegra S and Ballesta JJ (1997) Differential expression of alpha-bungarotoxin-sensitive neuronal nicotinic receptors in adrenergic chromaffin cells: a role for transcription factor Egr-1. J Neurosci 17, 6554–6564. [PubMed: 9254668]

Dani JA (2015) Neuronal Nicotinic Acetylcholine Receptor Structure and Function and Response to Nicotine. Int Rev Neurobiol 124, 3–19. [PubMed: 26472524]

David R, Ciuraszkiewicz A, Simeone X, Orr-Urtreger A, Papke RL, McIntosh JM, Huck S and Scholze P (2010) Biochemical and functional properties of distinct nicotinic acetylcholine receptors in the superior cervical ganglion of mice with targeted deletions of nAChR subunit genes. Eur J Neurosci 31, 978–993. [PubMed: 20377613]

de Diego AMG and Garcia AG (2018) Altered exocytosis in chromaffin cells from mouse models of neurodegenerative diseases. Acta Physiol (Oxf) 224, e13090. [PubMed: 29742321]

del Barrio L, Egea J, Leon R, Romero A, Ruiz A, Montero M, Alvarez J and Lopez MG (2011) Calcium signalling mediated through alpha7 and non-alpha7 nAChR stimulation is differentially regulated in bovine chromaffin cells to induce catecholamine release. Br J Pharmacol 162, 94–110. [PubMed: 20840468]

Di Angelantonio S, Matteoni C, Fabbretti E and Nistri A (2003) Molecular biology and electrophysiology of neuronal nicotinic receptors of rat chromaffin cells. Eur J Neurosci 17, 2313–2322. [PubMed: 12814364]

Douglas WW (1968) Stimulus-secretion coupling: the concept and clues from chromaffin and other cells. Br J Pharmacol 34, 451–474. [PubMed: 4882190]

Douglas WW, Kanno T and Sampson SR (1967) Effects of acetylcholine and other medullary secretagogues and antagonists on the membrane potential of adrenal chromaffin cells: an analysis employing techniques of tissue culture. J Physiol 188, 107–120. [PubMed: 4291730]

Douglas WW and Rubin RP (1961) The role of calcium in the secretory response of the adrenal medulla to acetylcholine. J Physiol 159, 40–57. [PubMed: 13887557]

Eiden LE, Emery AC, Zhang L and Smith CB (2018) PACAP signaling in stress: insights from the chromaffin cell. Pflugers Arch 470, 79–88. [PubMed: 28965274]

Eiden LE and Jiang SZ (2018) What's New in Endocrinology: The Chromaffin Cell. Front Endocrinol (Lausanne) 9, 711. [PubMed: 30564193]

El-Hajj RA, McKay SB and McKay DB (2007) Pharmacological and immunological identification of native alpha7 nicotinic receptors: evidence for homomeric and heteromeric alpha7 receptors. Life Sci 81, 1317–1322. [PubMed: 17928008]

Fuentealba J, Olivares R, Ales E et al. (2004) A choline-evoked [Ca2+]c signal causes catecholamine release and hyperpolarization of chromaffin cells. FASEB J 18, 1468–1470. [PubMed: 15231719]

Gahring LC, Myers E, Palumbos S and Rogers SW (2014) Nicotinic receptor Alpha7 expression during mouse adrenal gland development. PLoS One 9, e103861. [PubMed: 25093893]

Garcia AG, Garcia-De-Diego AM, Gandia L, Borges R and Garcia-Sancho J (2006) Calcium signaling and exocytosis in adrenal chromaffin cells. Physiol Rev 86, 1093–1131. [PubMed: 17015485]

Genzen JR, Van Cleve W and McGehee DS (2001) Dorsal root ganglion neurons express multiple nicotinic acetylcholine receptor subtypes. J Neurophysiol 86, 1773–1782. [PubMed: 11600638]

Gershon AS, Campitelli MA, Hawken S, Victor C, Sproule BA, Kurdyak P and Selby P (2018) Cardiovascular and Neuropsychiatric Events after Varenicline Use for Smoking Cessation. Am J Respir Crit Care Med 197, 913–922. [PubMed: 29260881]

Giribaldi J and Dutertre S (2018) alpha-Conotoxins to explore the molecular, physiological and pathophysiological functions of neuronal nicotinic acetylcholine receptors. Neurosci Lett 679, 24–34. [PubMed: 29199094]

Hajos M, Hurst RS, Hoffmann WE, Krause M, Wall TM, Higdon NR and Groppi VE (2005) The selective alpha7 nicotinic acetylcholine receptor agonist PNU-282987 [N-[(3R)-1-Azabicyclo[2.2.2]oct-3-yl]-4-chlorobenzamide hydrochloride] enhances GABAergic synaptic activity in brain slices and restores auditory gating deficits in anesthetized rats. J Pharmacol Exp Ther 312, 1213–1222. [PubMed: 15523001]

Hamelink C, Tjurmina O, Damadzic R, Young WS, Weihe E, Lee HW and Eiden LE (2002) Pituitary adenylate cyclase-activating polypeptide is a sympathoadrenal neurotransmitter involved in catecholamine regulation and glucohomeostasis. Proc Natl Acad Sci U S A 99, 461–466. [PubMed: 11756684]

Harrison-Woolrych M, Maggo S, Tan M, Savage R and Ashton J (2012) Cardiovascular events in patients taking varenicline: a case series from intensive postmarketing surveillance in New Zealand. Drug Saf 35, 33–43. [PubMed: 22149418]

Hone AJ, Fisher F, Christensen S, Gajewiak J, Larkin D, Whiteaker P and McIntosh JM (2019) PeIA-5466: A Novel Peptide Antagonist Containing Non-natural Amino Acids That Selectively Targets alpha3beta2 Nicotinic Acetylcholine Receptors. Journal of medicinal chemistry 62, 6262–6275. [PubMed: 31194549]

Hone AJ, McIntosh JM, Azam L, Lindstrom J, Lucero L, Whiteaker P, Passas J, Blazquez J and Albillos A (2015) alpha-Conotoxins Identify the alpha3beta4* Subtype as the Predominant Nicotinic Acetylcholine Receptor Expressed in Human Adrenal Chromaffin Cells. Mol Pharmacol 88, 881–893. [PubMed: 26330550]

Hone AJ, Meyer EL, McIntyre M and McIntosh JM (2012a) Nicotinic acetylcholine receptors in dorsal root ganglion neurons include the alpha6beta4* subtype. FASEB J 26, 917–926. [PubMed: 22024738]

Hone AJ, Michael McIntosh J, Rueda-Ruzafa L, Passas J, de Castro-Guerín C, Blázquez J, González-Enguita C and Albillos A (2017) Therapeutic concentrations of varenicline in the presence of nicotine increase action potential firing in human adrenal chromaffin cells. Journal of Neurochemistry 140, 37–52. [PubMed: 27805736]

Hone AJ, Ruiz M, Scadden M, Christensen S, Gajewiak J, Azam L and McIntosh JM (2013) Positional scanning mutagenesis of alpha-conotoxin PeIA identifies critical residues that confer potency and selectivity for alpha6/alpha3beta2beta3 and alpha3beta2 nicotinic acetylcholine receptors. J Biol Chem 288, 25428–25439. [PubMed: 23846688]

Hone AJ, Scadden M, Gajewiak J, Christensen S, Lindstrom J and McIntosh JM (2012b) alpha-Conotoxin PeIA[S9H,V10A,E14N] potently and selectively blocks alpha6beta2beta3 versus alpha6beta4 nicotinic acetylcholine receptors. Mol Pharmacol 82, 972–982. [PubMed: 22914547]

Hurst RS, Hajos M, Raggenbass M et al. (2005) A novel positive allosteric modulator of the alpha7 neuronal nicotinic acetylcholine receptor: in vitro and in vivo characterization. J Neurosci 25, 4396–4405. [PubMed: 15858066]

Kalappa BI, Gusev AG and Uteshev VV (2010) Activation of functional alpha7-containing nAChRs in hippocampal CA1 pyramidal neurons by physiological levels of choline in the presence of PNU-120596. PLoS One 5, e13964. [PubMed: 21103043]

Kanczkowski W, Sue M, Zacharowski K, Reincke M and Bornstein SR (2015) The role of adrenal gland microenvironment in the HPA axis function and dysfunction during sepsis. Mol Cell Endocrinol 408, 241–248. [PubMed: 25543020]

Kuri BA, Chan SA and Smith CB (2009) PACAP regulates immediate catecholamine release from adrenal chromaffin cells in an activity-dependent manner through a protein kinase C-dependent pathway. J Neurochem 110, 1214–1225. [PubMed: 19508428]

Lind MJ, Marraccini ME, Sheerin CM, Bountress K, Bacanu SA, Amstadter AB and Nugent NR (2017) Association of Posttraumatic Stress Disorder With rs2267735 in the ADCYAP1R1 Gene: A Meta-Analysis. J Trauma Stress 30, 389–398. [PubMed: 28746747]

Livak KJ and Schmittgen TD (2001) Analysis of relative gene expression data using real-time quantitative PCR and the 2(-Delta Delta C(T)) Method. Methods 25, 402–408. [PubMed: 11846609]

Livett BG, Boksa P, Dean DM, Mizobe F and Lindenbaum MH (1983) Use of isolated chromaffin cells to study basic release mechanisms. J Auton Nerv Syst 7, 59–86. [PubMed: 6188774]

Lopez MG, Montiel C, Herrero CJ et al. (1998) Unmasking the functions of the chromaffin cell alpha7 nicotinic receptor by using short pulses of acetylcholine and selective blockers. Proc Natl Acad Sci U S A 95, 14184–14189. [PubMed: 9826675]

Luo S, Zhangsun D, Zhu X et al. (2013) Characterization of a novel alpha-conotoxin TxID from Conus textile that potently blocks rat alpha3beta4 nicotinic acetylcholine receptors. Journal of medicinal chemistry 56, 9655–9663. [PubMed: 24200193]

Mahapatra S, Calorio C, Vandael DH, Marcantoni A, Carabelli V and Carbone E (2012) Calcium channel types contributing to chromaffin cell excitability, exocytosis and endocytosis. Cell Calcium 51, 321–330. [PubMed: 22317919]

Mao D, Yasuda RP, Fan H, Wolfe BB and Kellar KJ (2006) Heterogeneity of nicotinic cholinergic receptors in rat superior cervical and nodose Ganglia. Mol Pharmacol 70, 1693–1699. [PubMed: 16882879]

McIntosh JM, Azam L, Staheli S, Dowell C, Lindstrom JM, Kuryatov A, Garrett JE, Marks MJ and Whiteaker P (2004) Analogs of alpha-conotoxin MII are selective for alpha6-containing nicotinic acetylcholine receptors. Mol Pharmacol 65, 944–952. [PubMed: 15044624]

Mihalak KB, Carroll FI and Luetje CW (2006) Varenicline is a partial agonist at alpha4beta2 and a full agonist at alpha7 neuronal nicotinic receptors. Mol Pharmacol 70, 801–805. [PubMed: 16766716]

Mizobe F and Livett BG (1983) Nicotine stimulates secretion of both catecholamines and acetylcholinesterase from cultured adrenal chromaffin cells. J Neurosci 3, 871–876. [PubMed: 6834109]

Neher E and Marty A (1982) Discrete changes of cell membrane capacitance observed under conditions of enhanced secretion in bovine adrenal chromaffin cells. Proc Natl Acad Sci U S A 79, 6712–6716. [PubMed: 6959149]

Olsen JA, Kastrup JS, Peters D, Gajhede M, Balle T and Ahring PK (2013) Two distinct allosteric binding sites at alpha4beta2 nicotinic acetylcholine receptors revealed by NS206 and NS9283 give unique insights to binding activity-associated linkage at Cys-loop receptors. J Biol Chem 288, 35997–36006. [PubMed: 24169695]

Pardi D and Margiotta JF (1999) Pituitary adenylate cyclase-activating polypeptide activates a phospholipase C-dependent signal pathway in chick ciliary ganglion neurons that selectively inhibits alpha7-containing nicotinic receptors. J Neurosci 19, 6327–6337. [PubMed: 10414962]

Perez-Alvarez A and Albillos A (2007) Key role of the nicotinic receptor in neurotransmitter exocytosis in human chromaffin cells. J Neurochem 103, 2281–2290. [PubMed: 17883397]

Perez-Alvarez A, Hernandez-Vivanco A, Cano-Abad M and Albillos A (2008) Pharmacological and biophysical properties of Ca2+ channels and subtype distributions in human adrenal chromaffin cells. Pflugers Arch 456, 1149–1162. [PubMed: 18443816]

Perez-Alvarez A, Hernandez-Vivanco A, Gregorio SA, Tabernero A, McIntosh JM and Albillos A (2012) Pharmacological characterization of native alpha7 nAChRs and their contribution to depolarization-elicited exocytosis in human chromaffin cells. Br J Pharmacol 165, 908–921. [PubMed: 21790533]

Podvin S, Bundey R, Toneff T, Ziegler M and Hook V (2015) Profiles of secreted neuropeptides and catecholamines illustrate similarities and differences in response to stimulation by distinct secretagogues. Mol Cell Neurosci 68, 177–185. [PubMed: 26092702]

Rau KK, Johnson RD and Cooper BY (2005) Nicotinic AChR in subclassified capsaicin-sensitive and -insensitive nociceptors of the rat DRG. J Neurophysiol 93, 1358–1371. [PubMed: 15483069]

Ressler KJ, Mercer KB, Bradley B et al. (2011) Post-traumatic stress disorder is associated with PACAP and the PAC1 receptor. Nature 470, 492–497. [PubMed: 21350482]

Rollema H, Shrikhande A, Ward KM et al. (2010) Pre-clinical properties of the alpha4beta2 nicotinic acetylcholine receptor partial agonists varenicline, cytisine and dianicline translate to clinical efficacy for nicotine dependence. Br J Pharmacol 160, 334–345. [PubMed: 20331614]

Sala F, Nistri A and Criado M (2008) Nicotinic acetylcholine receptors of adrenal chromaffin cells. Acta Physiol (Oxf) 192, 203–212. [PubMed: 18005395]

Singh S, Loke YK, Spangler JG and Furberg CD (2011) Risk of serious adverse cardiovascular events associated with varenicline: a systematic review and meta-analysis. CMAJ 183, 1359–1366. [PubMed: 21727225]

Smith NJ, Hone AJ, Memon T, Bossi S, Smith TE, McIntosh JM, Olivera BM and Teichert RW (2013) Comparative functional expression of nAChR subtypes in rodent DRG neurons. Front Cell Neurosci 7, 225. [PubMed: 24348328]

Stokes C and Papke RL (2012) Use of an alpha3beta4 nicotinic acetylcholine receptor subunit concatamer to characterize ganglionic receptor subtypes with specific subunit composition reveals species-specific pharmacologic properties. Neuropharmacology 63, 538–546. [PubMed: 22580377]

Stroth N, Kuri BA, Mustafa T, Chan SA, Smith CB and Eiden LE (2013) PACAP controls adrenomedullary catecholamine secretion and expression of catecholamine biosynthetic enzymes at high splanchnic nerve firing rates characteristic of stress transduction in male mice. Endocrinology 154, 330–339. [PubMed: 23221599]

Whiteaker P, Christensen S, Yoshikami D, Dowell C, Watkins M, Gulyas J, Rivier J, Olivera BM and McIntosh JM (2007) Discovery, synthesis, and structure activity of a highly selective alpha7 nicotinic acetylcholine receptor antagonist. Biochemistry 46, 6628–6638. [PubMed: 17497892]

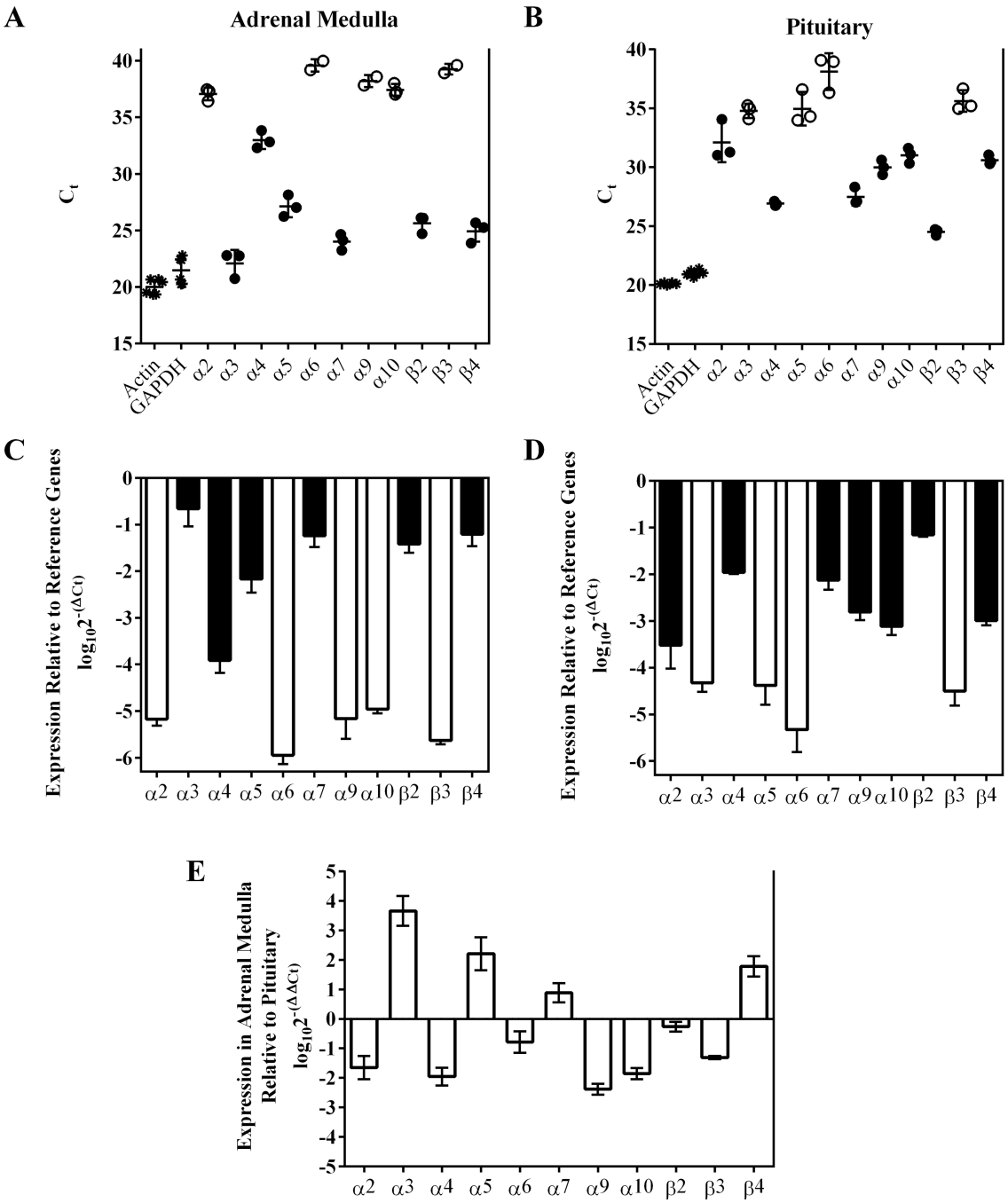

Figure 1.

qPCR of rat adrenal medulla and pituitary gland reveals the expression of mRNAs for multiple nAChR subunits. Isolated mRNA from three rat adrenal medulla and three pituitary glands from the same animals were analyzed by qPCR as described in Methods. Panel (A) shows the C_t values for the mRNAs assayed in adrenal medulla. Each data point represents the average of three technical repeats for each gene from a single animal except for α6, α9, and β3 subunit. For α6 and β3 subunits, mRNA was only detected in two of three animals and signal was not detected in every technical repeat. For α9 subunits, signal reached

threshold for two of three animals. Panel B shows the C_t values for the mRNAs present in pituitary. Each data point represents the average of three technical repeats for each gene from a single animal. Closed circles in A and B indicate average C_t values ≤35 whereas open circles indicate values >35. Panels C and D show the expression levels of nAChR subunit mRNAs relative to those of the reference genes actin and GAPDH; panel C is for adrenal medulla and D is for pituitary. (E) A pairwise comparison for each nAChR subunit gene of the relative expression levels present in adrenal medulla and pituitary. Positive values indicate higher levels of expression in the adrenal medulla and negative values indicate higher levels in the pituitary for each gene. The error bars in all graphs denote the SD; values and statistical comparisons are provided in Table 1.

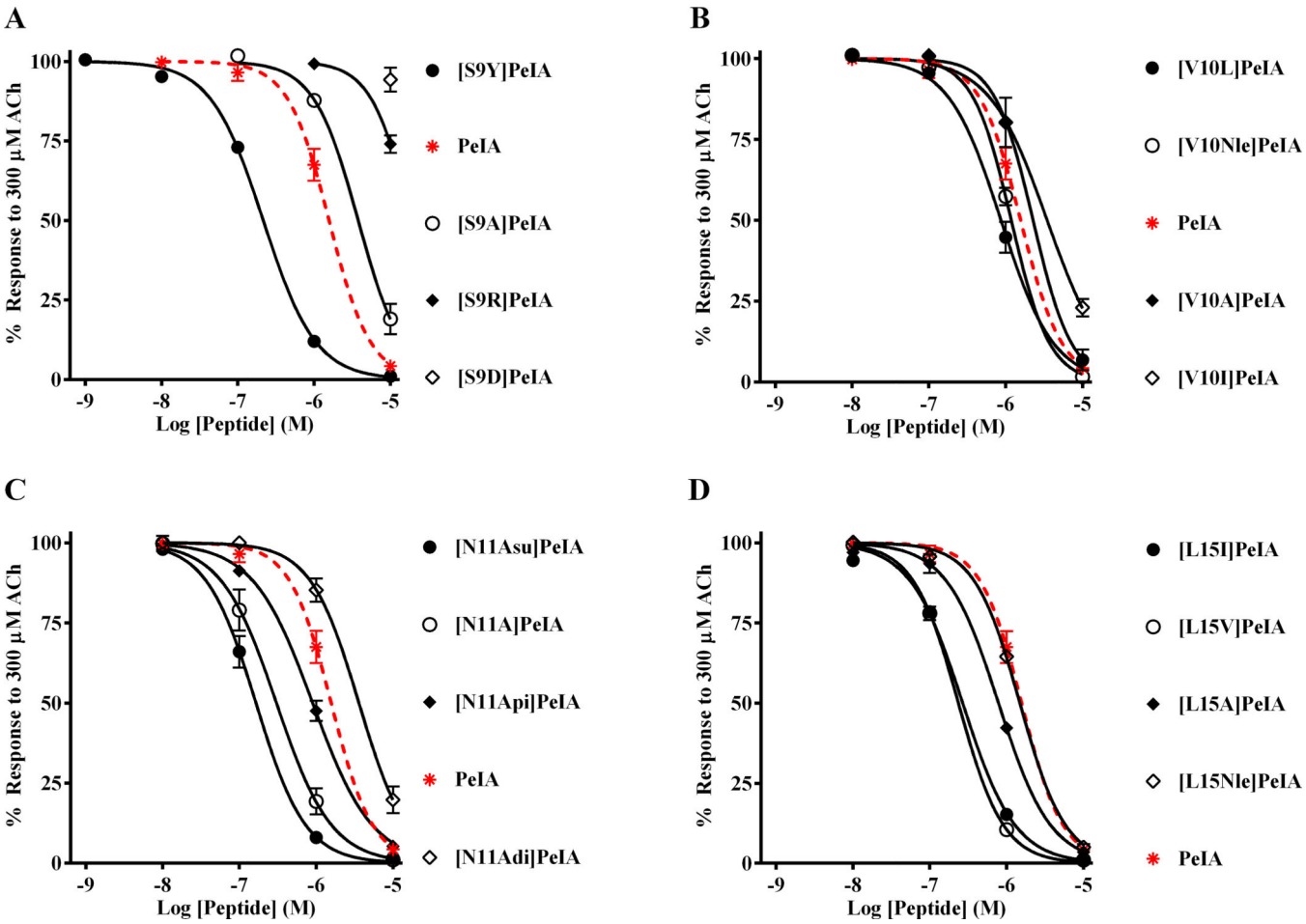

Figure 2.

Concentration-response curves for the inhibition of α3β4 nAChRs by PeIA and related analogs. Rat α3β4 nAChRs were heterologously expressed in *X. laevis* oocytes and the potencies of the peptides assessed using TEVC as described in Methods. The error bars indicate the SD of the data obtained from four oocytes for all IC_{50} curves except for that of [V10Nle]PeIA where an n of five was obtained; IC_{50} values are provided in Table 2.

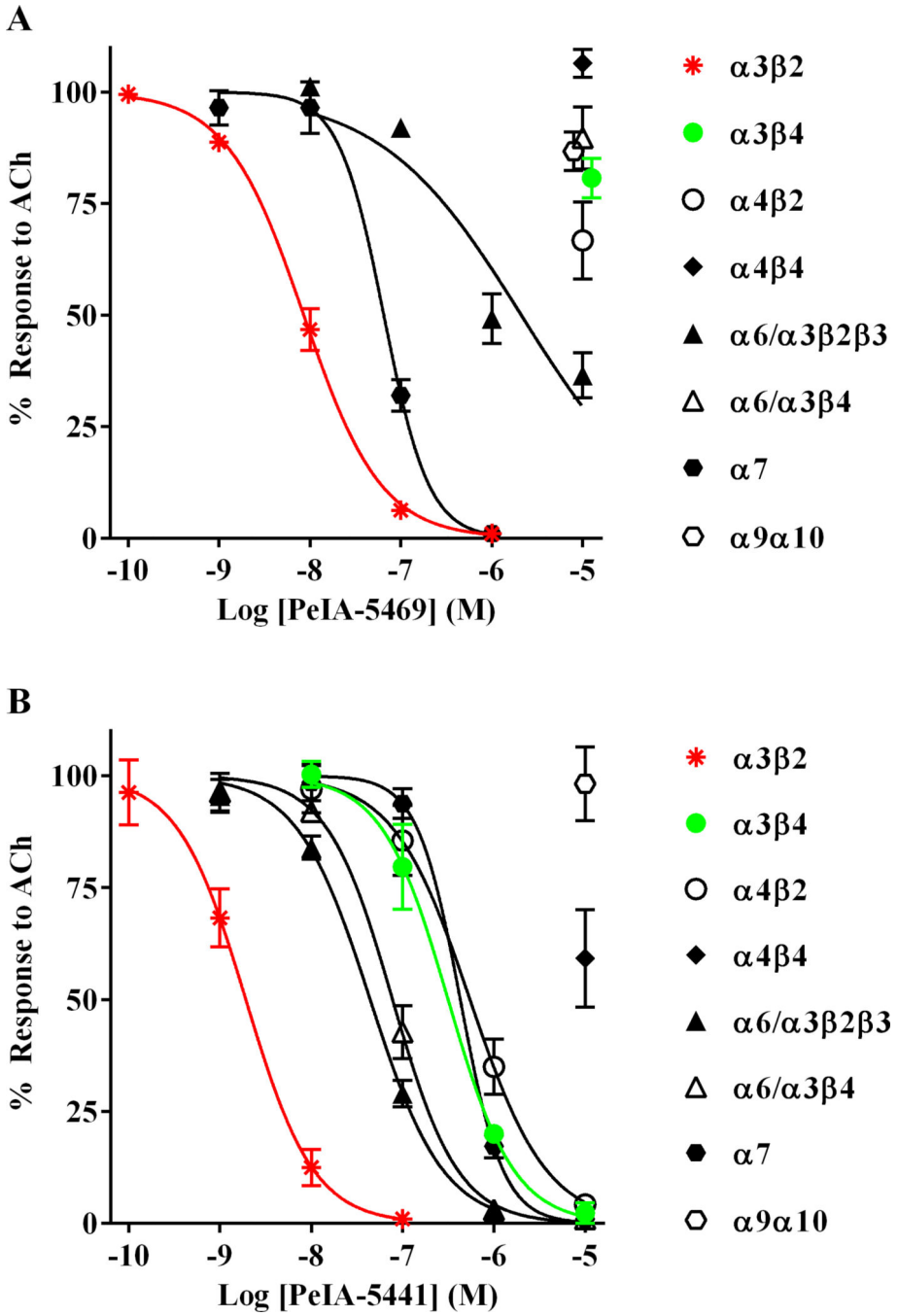

Figure 3.

Concentration-response analysis for PeIA-5469 and PeIA-5441 on a panel of nAChR subtypes heterologously expressed in *X. laevis* oocytes. The oocytes were subjected to TEVC electrophysiology and the potencies of the two PeIA analogs were assessed as described in Methods. (A) PeIA-5469 and (B) PeIA-5441 show different selectivity profiles despite being almost identical in sequence. The sequence of PeIA-5469 is GCCSHPACRI(Api)HPENleC and the sequence of PeIA-5441 is GCCSHPACHI(Api)HPENleC; (Api), α-amino pimelic acid. Note that both peptides are

highly selective for α3β2 over α3β4 nAChRs but PeIA-5469 showed the largest separation in IC_{50} values (1,175-fold vs. 198-fold, respectively). Data points for α3β4 and α9α10 in A are shown staggered to avoid overlap. The error bars represent the SD of the data obtained from four oocytes for all peptides except for that of PeIA-5441 on α3β4 nAChRs where an n of three was obtained; IC_{50} values are provided in Table 3.

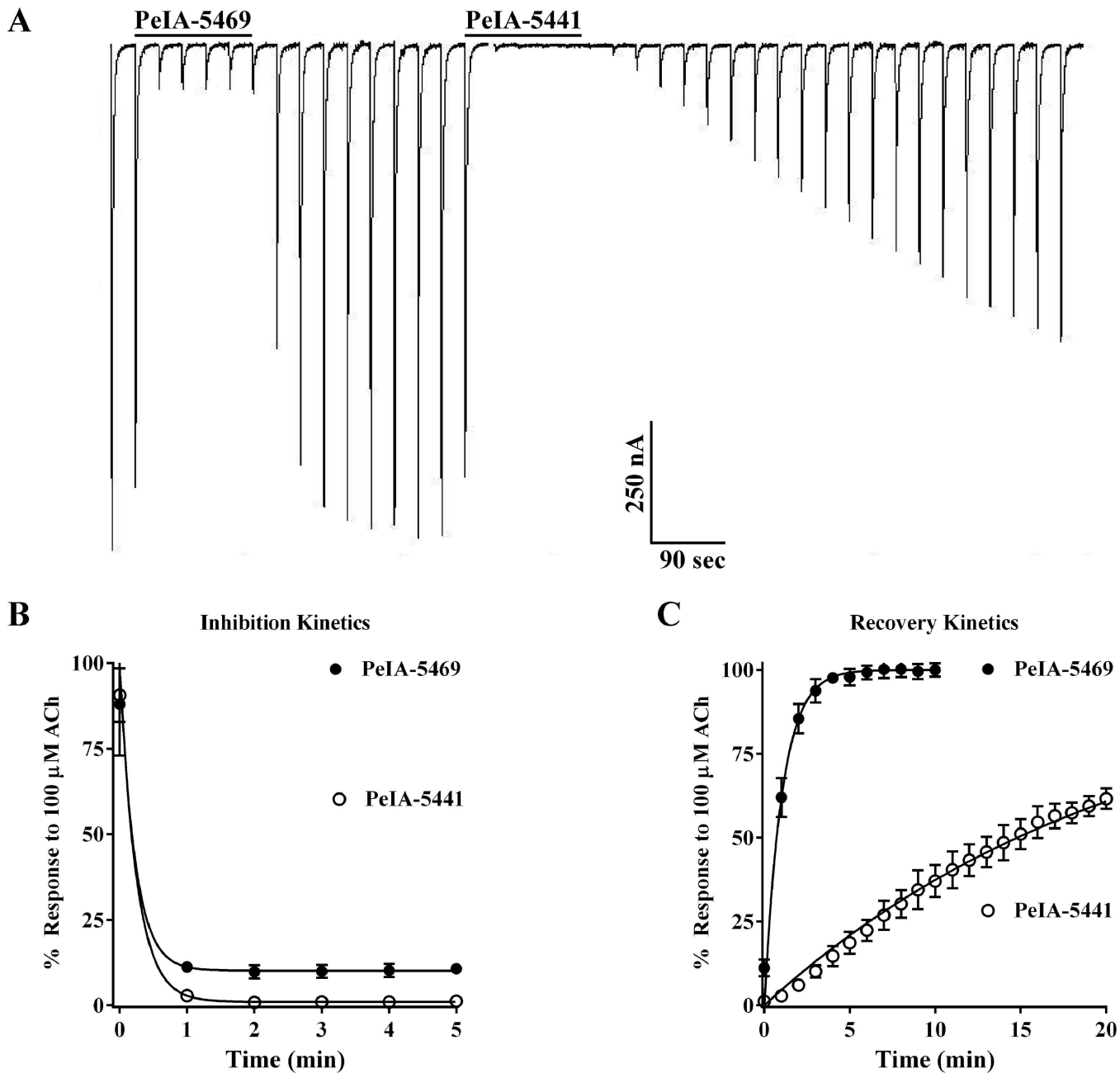

Figure 4.

Kinetic analysis of the inhibition of α3β2 nAChRs by PeIA-5469 and PeIA-5441. *X. laevis* oocytes were subjected to TEVC electrophysiology as described in Methods and the inhibition and recovery kinetics of PeIA-5469 and PeIA-5441 were assessed. (A) Representative current traces of ACh-evoked responses from an oocyte expressing α3β2 nAChRs before, during, and after the sequential exposure to PeIA-5469 and PeIA-5441. (B) Graph showing the time-course for inhibition by the two peptides. Note that for the concentration used (100 nM for both), equilibrium was reached in less than two minutes after exposure to the peptides preventing quantitative analysis of inhibition-rate kinetics under these experimental conditions. (C) Graph showing the time-course for recovery of the

responses after washout of the peptides. The $t_{1/2}$ for recovery after exposure to PeIA-5469 was significantly shorter than that for PeIA-5441 (0.8 ± 0.2 vs 22.2 ± 11.5 min; n=4 for both; **p≤0.01, Student's *t*-test). The error bars in B and C indicate the SD; 'n' values indicate the number of oocytes assessed.

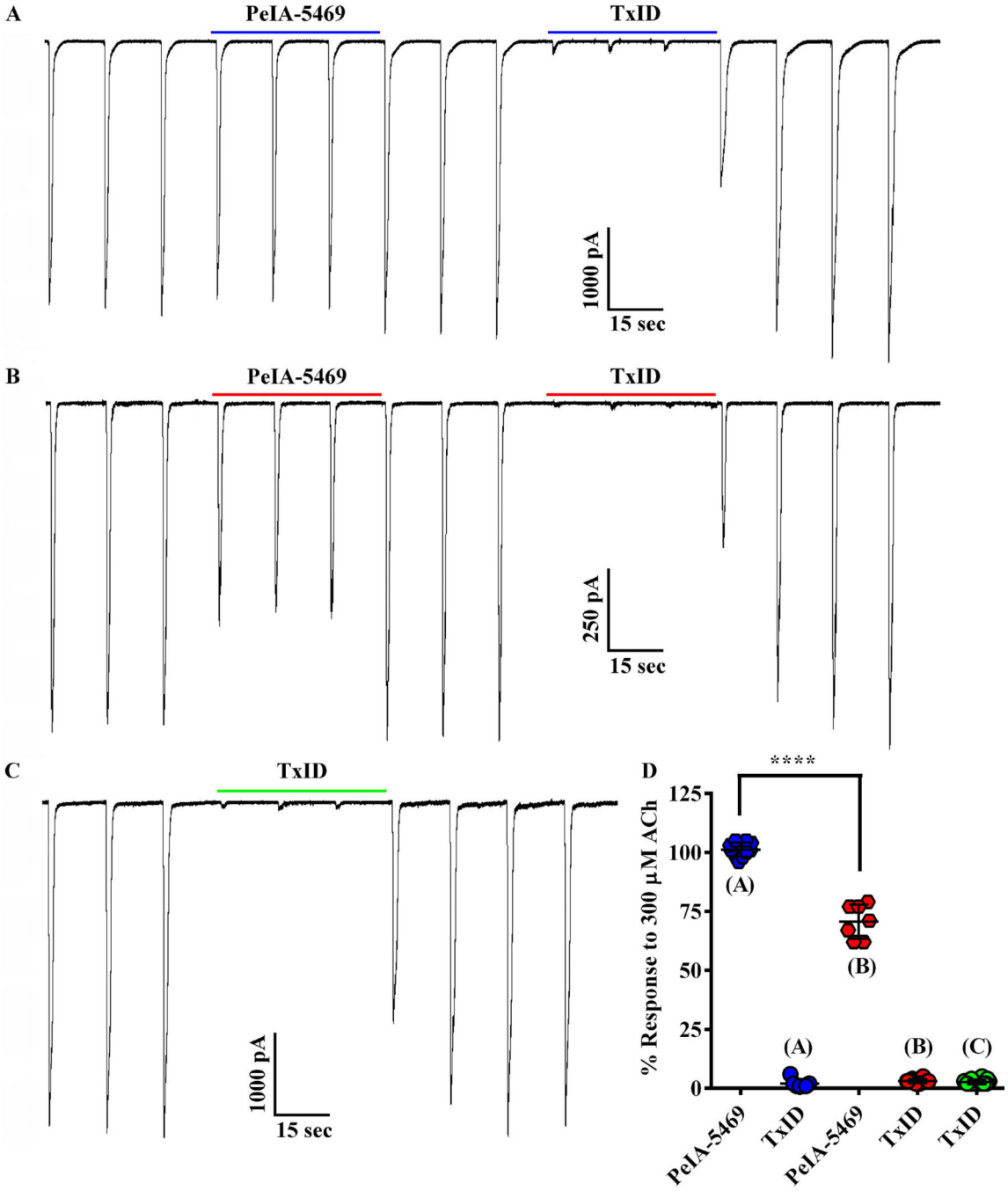

Figure 5.

Presence of α3β2β4 and α3β4 nAChRs in rat adrenal chromaffin cells demonstrated using subtype-selective α-conotoxin antagonists. (A and B) Traces of ACh-evoked currents before, during, and after exposure to PeIA-5469 (100 nM) and TxID (1 μM). In the population of cells (n=10) represented in A, the ACh-evoked currents in the presence of PeIA-5469 were 101 ± 3% of controls and 3 ± 1% in the presence of TxID. By contrast, in the population of cells (n=7) represented in B, the ACh-evoked currents in the presence of PeIA-5469 were 71 ± 7% of controls and 3 ± 1% in the presence of TxID. Currents in the presence of

PeIA-5469 were significantly smaller than controls (−1500 ± 705 pA vs −2073 ± 805 pA, respectively; ****p ≤ 0.0001, *t*-test). The % response in the presence of PeIA-5469 in B was significantly smaller (****p ≤ 0.0001, *t*-test) compared to A. (C) Traces of ACh-evoked currents in a cell exposed to TxID only. There was no statistically significant difference for the level of inhibition produced by exposure to TxID only (C) or exposure to TxID after exposure to PeIA-5469 (A and B); p>0.05, *t*-test). All solutions contained [V11L,V16D]ArIB (100 nM) to inhibit any α7 nAChRs that might be present. (D) Scatter plot of the data from A-C. The error bars in D and all '±' values indicate the SD; 'n' values indicate number of cells obtained from three separate cell cultures.

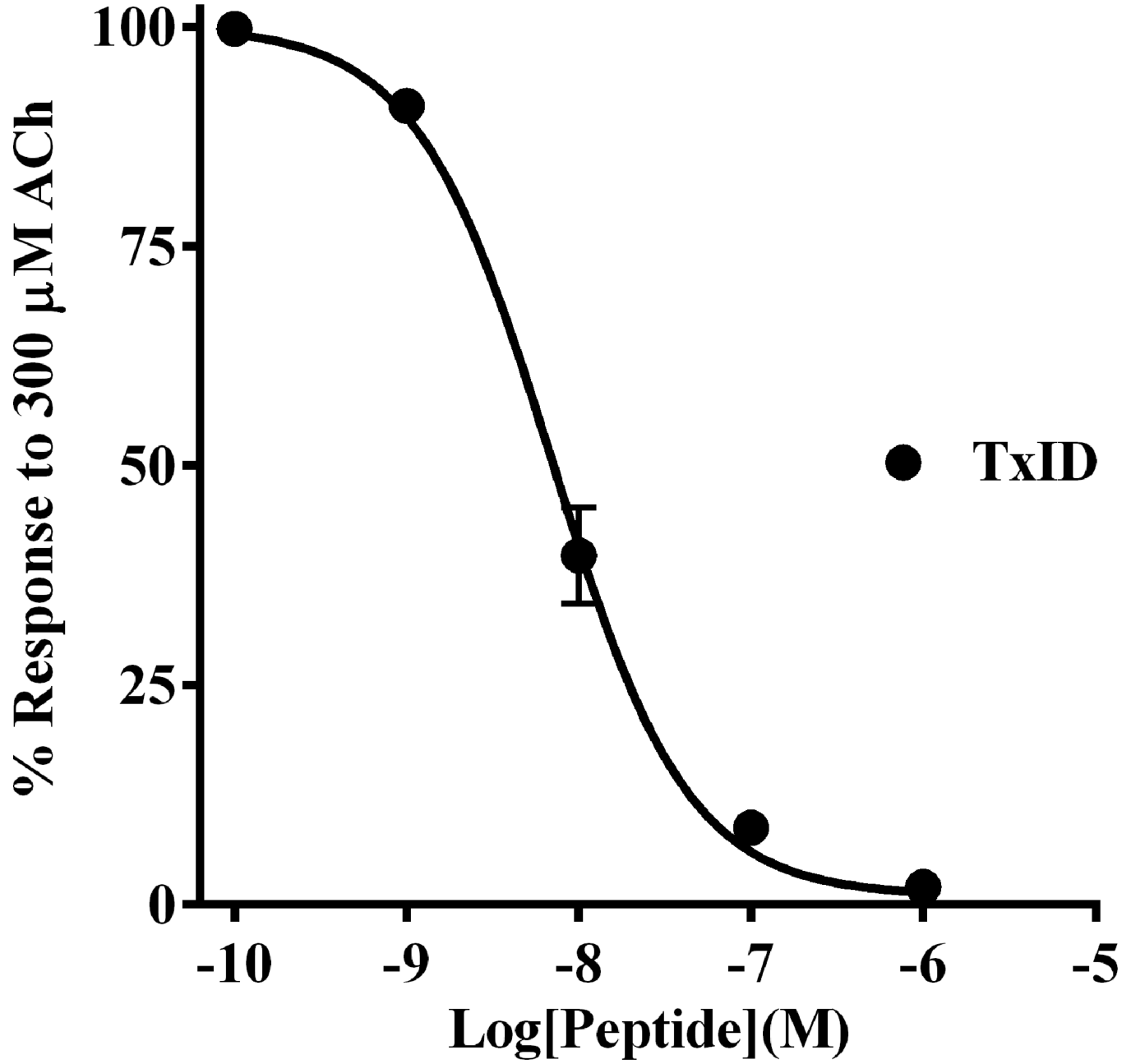

Figure 6.

Determination of TxID potency on native α3β4* nAChRs expressed by rat adrenal chromaffin cells. Adrenal chromaffin cells were cultured and subjected to patch-clamp electrophysiology as described in Methods. The cells were stimulated with ACh (300 μM) and then perfused with increasing concentrations of TxID. Analysis of the data determined that the IC_{50} value of the peptide for inhibition of ACh-evoked currents was 7.0 (6.3–7.8) nM (n=4). The Hill slope was −1.1 (−1.2 to −1.0). Values in parenthesis indicate the 95% confidence interval and the error bars in the graph indicate the SD of the data; 'n' values indicate the number of cells from one cell culture. All solutions contained [V11L,V16D]ArIB (100 nM) to inhibit any α7 nAChRs that might be present.

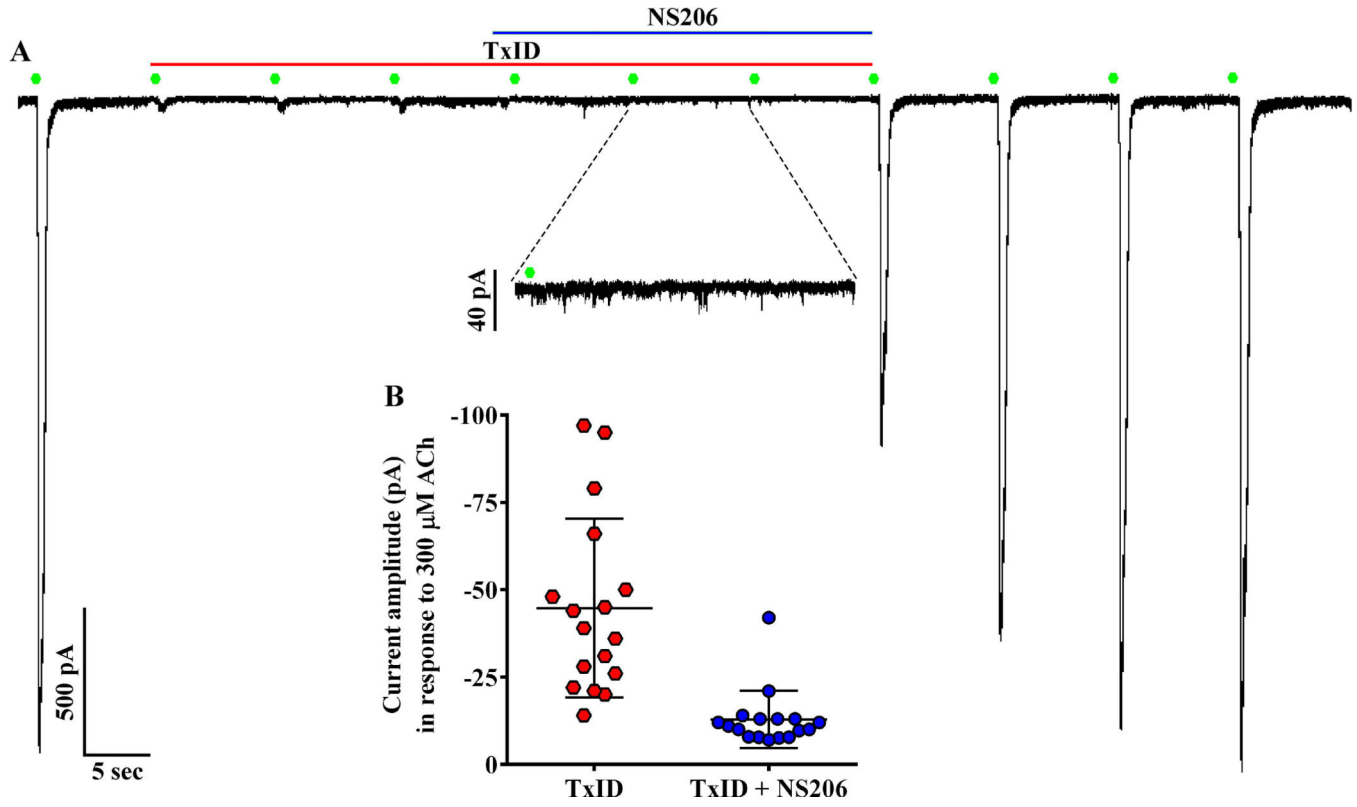

Figure 7.

Absence of α4β2 and α4β4 nAChRs demonstrated using the positive allosteric modulator (PAM) NS206. (A) Representative currents from a cell stimulated with ACh (300 µM, green symbols) and then exposed to NS206 (10 µM) in the presence of TxID (1 µM). (B) Scatter plot of the current amplitudes in the presence of TxID compared to those in the presence of TxID and NS206. Currents in the presence of TxID and NS206 were smaller than those in TxID alone (−13 ± 8 pA vs −45 ± 26 pA, respectively, n=17; ***p≤ 0.001, *t*-test). The '±' values and error bars in (B) indicate the SD; 'n' values indicate the number of cells obtained from two separate cell cultures. All solutions contained [V11L,V16D]ArIB (100 nM) to inhibit any α7 nAChRs that might be present.

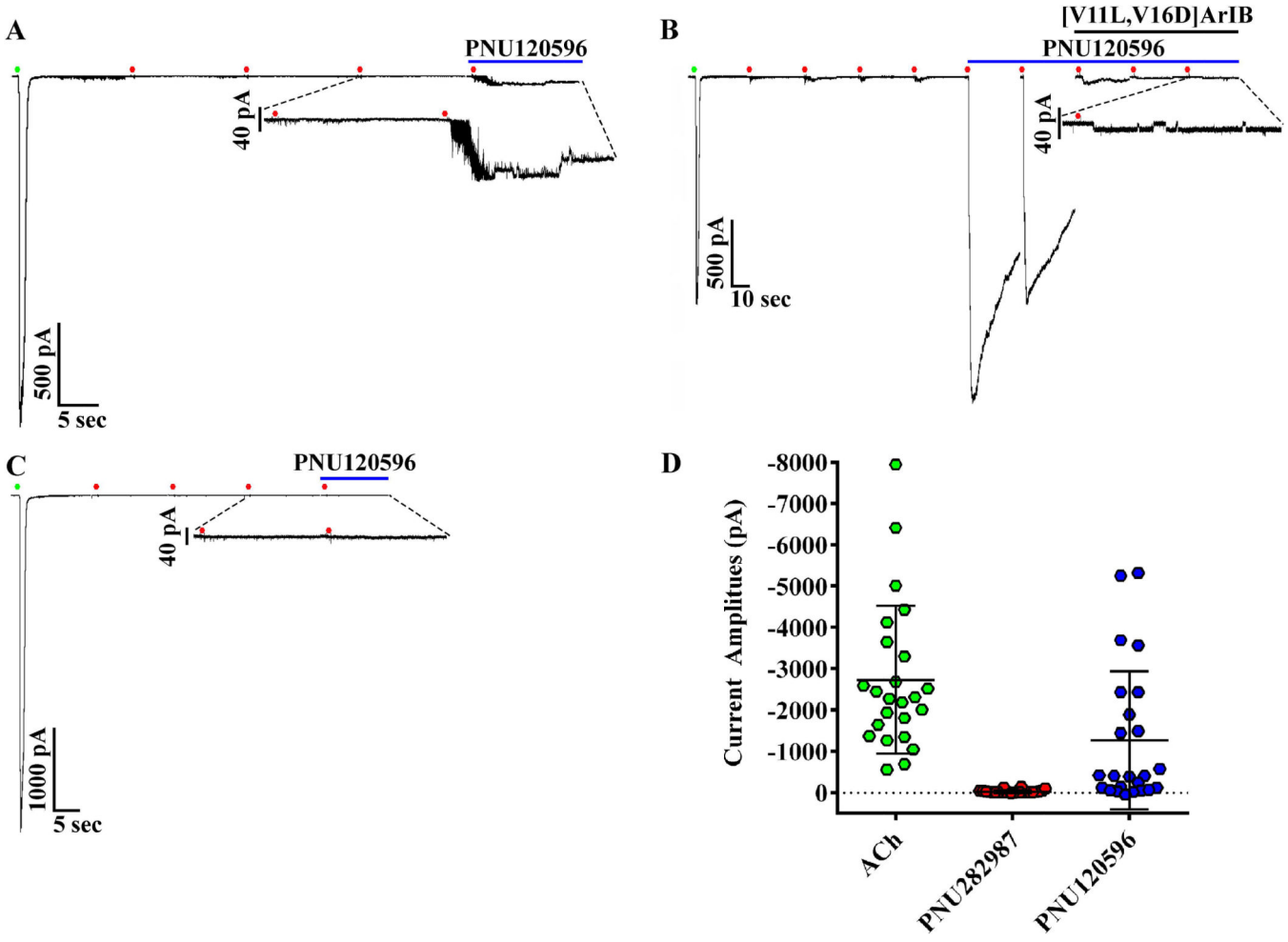

Figure 8.

Presence of functional α7 nAChRs demonstrated using three α7-selective ligands. (A-C) Currents from cells stimulated with ACh (300 μM, green symbols) then with the agonist PNU282987 (30 μM, red symbols) followed by exposure to the PAM PNU120596 (3 μM). (A-B) PNU282987-evoked currents (−36 ± 41 pA) were observed in 18/28 cells. Stimulation of the cells with PNU282987 in the presence of PNU120596 resulted in a 54 ± 99-fold increase in current amplitudes (−29 ± 38 pA to −1275 ± 1668 pA; ****$p \leq 0.0001$, Wilcoxon Signed Rank test) in 24/28 cells including six cells (A) that initially showed no response to PNU282987. (B) Exposure to the antagonist [V11L,V16D]ArIB (300 nM) reduced the modulated currents to 2 ± 2% of controls in 10/10 cells in which the antagonist was applied. (C) In 4/28 cells exposed to PNU120596, no PNU282987-evoked currents were observed (−4.5 ± 0.4 pA vs −3.9 ± 1.2 pA, respectively). (D) Scatter plot showing the current amplitudes evoked by ACh compared to PNU282987 and the currents evoked by PNU282987 in the presence of the PNU120596. The ACh-evoked currents in these cells were −2730 ± 1789 pA (n=24). Data are from cells that responded to PNU120596. The '±' values and the error bars in (D) indicate the SD; 'n' values indicate the number of cells obtained from three separate cell cultures.

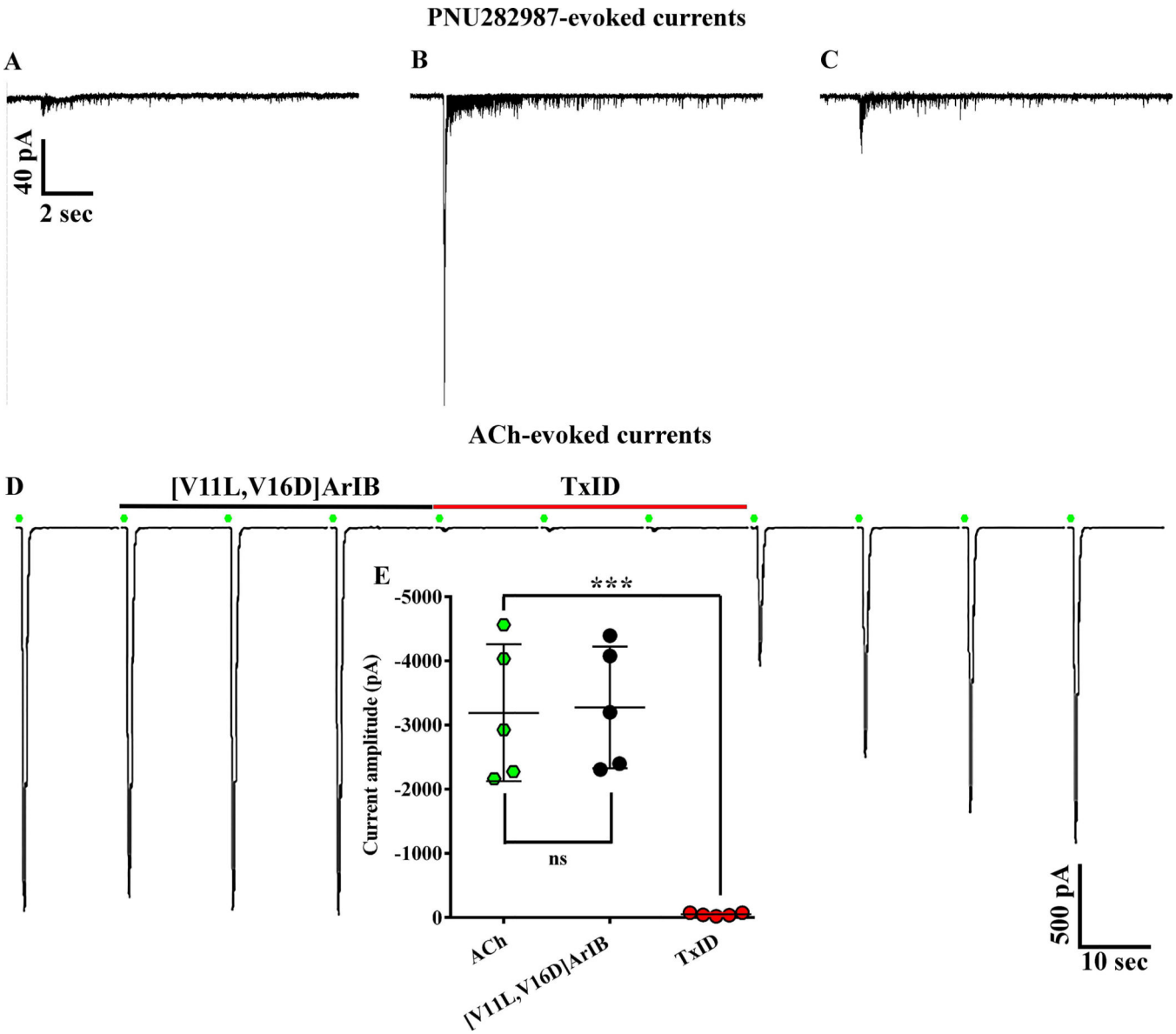

Figure 9.

Lack of effect by [V11L,V16D]ArIB on ACh-evoked currents. (A-C) Examples of small, large, and mean amplitude currents evoked by PNU282987 (30 μM). PNU282987-evoked currents were substantially smaller than those evoked by ACh (300 μM) in the same cells (−37 ± 57 pA vs −3992 ± 1649 pA, respectively; n=7). (D) ACh-evoked currents (green symbols) before, during, and after exposure to [V11L,V16D]ArIB (100 nM) followed by TxID (1 μM). ACh-evoked currents in the presence of [V11L,V16D]ArIB were 102 ± 4% of controls and reduced to 2 ± 1% in the presence of TxID (n=5). (E) Currents in the presence of [V11L,V16D]ArIB (−3275 ± 949 pA) were no different than controls (−3193 ± 1067 pA, n=5; $p > 0.05$, *t*-test). By contrast, those in the presence of TxID (−50 ± 24 pA) were significantly smaller (n=5; ** $p \leq 0.01$, *t*-test). Current traces in C and D are from the same

cell. The ‘±’ values and error bars indicate the SD; n values indicate the number of cells obtained from one cell culture.

TABLE 1.

qPCR analysis of nAChR subunit gene expression in rat adrenal medulla and pituitary gland

	Adrenal Medulla				Pituitary			Adrenal Medulla relative to Pituitary	
Gene	**C_t**	**n**	**$\log_{10}2^{-(\Delta Ct)}$**	**Fold-less relative to α3**	**C_t**	**n**	**$\log_{10}2^{-(\Delta Ct)}$**	**$\log_{10}2^{-(\Delta\Delta Ct)}$**	**Fold-difference**
actin	20.0 ± 0.7	6	nd	nd	20.1 ±0.09	6	nd	nd	nd
GAPDH	21.5 ± 1.2	6	nd	nd	21.0 ± 0.2	6	nd	nd	nd
α2	37.1 ± 0.6	3	−5.2 ± 0.1	>30,000 ****	32.2 ± 1.7	3	−3.5 ± 0.5	−1.7 ± 0.4	−44.7 ± 2.5 ****
α3	22.1 ± 1.2	3	−0.7 ± 0.4	1	34.8 ± 0.6	3	−4.3 ± 0.2	3.7 ± 0.5	4,602 ± 3 ****
α4	33.0 ± 0.8	3	−3.9 ± 0.3	>1,500 ****	29.6 ± 0.2	3	−2.0 ± 0.04	−1.9 ± 0.3	−89.7 ± 2.0 ****
α5	27.1 ± 1.0	3	−2.2 ± 0.3	32 ± 1.6 ****	35.0 ± 1.4	3	−4.4 ± 0.4	2.2 ± 0.6	163 ± 4 ****
α6	39.6 ± 0.6	2	−5.9 ± 0.2	>150,000 ****	38.1 ± 1.6	3	−5.3 ± 0.5	−0.8 ± 0.4	−4.2 ± 2.3 *ns*
α7	24.0 ± 0.7	3	−1.2 ± 0.2	3.8 ± 1.6 *ns*	27.5 ± 0.7	3	−2.2 ± 0.2	0.9 ± 0.3	7.7 ± 2.1 *
α9	38.2 ± 0.5	2	−5.2 ± 0.4	>30,000 ****	30.0 ± 0.6	3	−2.8 ± 0.2	−2.4 ± 0.2	−228 ± 1.5 ****
α10	37.4 ± 0.5	3	−5.0 ± 0.08	>20,000 ****	31.0 ± 0.6	3	−3.1 ± 0.2	−1.9 ± 0.2	−70.8 ± 1.5 ****
β2	25.6 ± 0.8	3	−1.4 ± 0.2	5.7 ± 1.6 *	24.5 ± 0.3	3	−1.2 ± 0.04	−0.3 ± 0.2	−1.8 ± 1.5 *ns*
β3	39.3 ± 0.5	2	−5.6 ± 0.08	>90,000 ****	35.6 ± 0.9	3	−4.5 ± 0.3	−1.3 ± 0.06	−13.5 ± 0.3 **
β4	24.9 ± 0.9	3	−1.2 ± 0.3	3.5 ± 1.6 *ns*	30.6 ± 0.4	3	−3.0 ± 0.1	1.8 ± 0.3	61.2 ± 2.1 ****

Tissues from three animals were analyzed individually. Positive values for comparisons of gene expression between adrenal medulla and pituitary indicate greater relative abundance in the adrenal medulla. Significance was determined using a one-way ANOVA with a Holm-Šídák post hoc comparison test

ns not significant or $p > 0.05$

* $p \leq 0.05$

** $p \leq 0.01$

*** $p \leq 0.001$

**** $p \leq 0.0001$

'±' values indicate the SD; C_t, cycle threshold; fold-less and fold-difference values were converted from logarithmic units; 'n' values indicate number of tissue samples where the reaction reached threshold; inclusion of actin and GAPDH reactions in two separate runs resulted in higher n values and were included in each run to ensure plate-to-plate reproducibility of results.

TABLE 2.

IC_{50} values for PeIA and analogs with single substitutions on α3β4 nAChRs expressed in X. laevis oocytes.

Peptide	IC_{50} value (μM)	Log change in IC_{50} relative to PeIA
PeIA	1.57 (1.28–1.92)	-
[S9A]PeIA	3.79 (3.01–4.78)	0.4
[S9R]PeIA	18.7 (5.09–68.9)	1.1
[S9D]PeIA	> 10	> 0.8
[S9Y]PeIA	0.22 (0.20–0.27)	−0.9
[V10I]PeIA	3.47 (2.30–5.24)	0.3
[V10L]PeIA	0.87 (0.71–1.05)	−0.3
[V10Nle]PeIA	1.18 (1.08–1.29)	−0.1
[N11A]PeIA	0.30 (0.23–0.41)	−0.7
[N11Adi]PeIA	3.60 (2.91–4.46)	0.4
[N11Api]PeIA	0.90 (0.78–1.04)	−0.2
[N11Asu]PeIA	0.16 (0.13–0.20)	−1.0
[L15A]PeIA	0.78 (0.68–0.91)	−0.3
[L15V]PeIA	0.24 (0.21–0.26)	−0.8
[L15I]PeIA	0.27 (0.24–0.30)	−0.8
[L15Nle]PeIA	1.49 (1.34–1.65)	−0.1

Values in parentheses indicate the 95% CI; negative log values indicate increased potency and positive values indicate decreased potency relative to native PeIA.

TABLE 3.

Potencies of PeIA-5469 and PeIA-5441 for nAChR subtypes expressed in X. laevis oocytes

	IC_{50} values (nM)							
	α3β2	**α3β4**	**α4β2**	**α4β4**	**α6/α3β2β3**	**α6/α3β4**	**α7**	**α9α10**
PeIA-5469	8.5 (7.8–9.4)	>10,000	>10,000	>10,000	2,110 (1,250–3,581)	>10,000	6.5 (5.5–7.6)	>10,000
PeIA-5441	1.9 (1.6–2.3)	316 (253–394)	548 (442–648)	>10,000	44.2 (39.2–49.7)	77.7 (69.2–87.1)	42.9 (37.8–48.7)	>10,000

Values in parentheses indicate the 95% CI.

TABLE 4.

Potencies of TxID and [V11L,V16D]ArIB for nAChR subtypes expressed in X. laevis oocytes

	IC_{50} values (nM)							
	α3β2	**α3β4**	**α4β2**	**α4β4**	**α6/α3β2β3**	**α6/α3β4**	**α7**	**α9α10**
TxID	>10,000[a]	12.5[a]	>10,000[a]	>10,000[a]	>10,000[a]	94.1[a]	>10,000[a]	>10,000[a]
[V11L,V16D]ArIB	>10,000[b]	>10,000[b]	>10,000 [b]	>10,000 [b]	828 [b]	>10,000 [b]	1.09[b]	>10,000[b]

[a] Luo et al., 2012

[b] Whiteaker et al., 2007